Geophysical Journal International

*Geophys. J. Int.* (2015) **201,** 683–710 doi: 10.1093/gji/ggv005
GJI Geodynamics and tectonics

# Evolution and dynamics of a fold-thrust belt: the Sulaiman Range of Pakistan

Kirsty Reynolds,[1] Alex Copley[1] and Ekbal Hussain[2]

[1]*COMET, Bullard Labs, Department of Earth Sciences, University of Cambridge, Cambridge, United Kingdom. E-mail: kr374@cam.ac.uk*
[2]*COMET, School of Earth and Environment, University of Leeds, Leeds, United Kingdom*

Accepted 2015 January 5. Received 2015 January 4; in original form 2014 June 10

## SUMMARY

We present observations and models of the Sulaiman Range of western Pakistan that shed new light on the evolution and deformation of fold-thrust belts. Earthquake source inversions show that the seismic deformation in the range is concentrated in the thick pile of sediments overlying the underthrusting lithosphere of the Indian subcontinent. The slip vectors of the earthquakes vary in strike around the margin of the range, in tandem with the shape of the topography, suggesting that gravitational driving forces arising from the topography play an important role in governing the deformation of the region. Numerical models suggest that the active deformation, and the extreme plan-view curvature of the range, are governed by the presence of weak sediments in a pre-existing basin on the underthrusting Indian Plate. These sediments affect the stress-state in the over-riding mountain range and allow for the rapid propagation of the nose of the range and the development of extreme curvature and laterally varying surface gradients.

**Key words:** Seismicity and tectonics; Continental neotectonics; Dynamics: gravity and tectonics; Dynamics: seismotectonics.



## 1 INTRODUCTION

Plan-view curvature of geological structures and range-front topography has long been a recognized and debated feature of both ancient and active fold-thrust belts (e.g. Argand 1924; Carey 1955; Hindle & Burkhard 1999; Marshak 2004). Though poorly understood, the relationship between the size and shape of a mountain range, surface deformation, and continental rheology, is key to our understanding of mountain-building processes. As the largest active mountain ranges on Earth, much of the body of work surrounding this topic has focused on the Tibetan Plateau and the Andes (e.g. Argand 1924; Suárez *et al.* 1983; Dewey *et al.* 1988; England & Houseman 1988; Isacks 1988; Molnar & Lyon-Caen 1989; Whitman *et al.* 1996; Lamb & Hoke 1997; Barke *et al.* 2007; Royden *et al.* 2008). However, a full understanding of continental tectonics and rheology requires knowledge of the deformation, evolution and dynamics of not just the planet's largest and most rapidly deforming regions, but also of smaller deformation zones (e.g. Batt & Braun 1999; Macedo & Marshak 1999; Nissen *et al.* 2011b). A lack of published data, extremely limited geodetic coverage and difficulty of access mean there have been relatively few studies of the western part of the Himalaya–Tibetan Plateau system, where the Himalaya curve to the southwest into the lobate fold-thrust belts of Pakistan. The widest of these, the Sulaiman Range (Fig. 1a), forms a strongly curved, asymmetric lobe with ∼300 km across-strike width. This range has experienced plentiful earthquakes during the instrumental period, and has been the subject of several competing hypotheses about the behaviour and mechanics of fold-thrust belts (Humayon *et al.* 1991; Jadoon & Khurshid 1996; Haq & Davis 1997; Macedo & Marshak 1999; Bernard *et al.* 2000; Reiter *et al.* 2011). In this paper, we study the Sulaiman Range in order to gain insights into the dynamics and evolution of the range, and the mechanics of curve formation.

We present source parameters determined by inversion of teleseismic body waves for 10 moderate-sized ($\geq M_w$5.2) earthquakes in the Sulaiman Range. Using these focal mechanisms and depths, along with observations of topography, seismicity, gravity anomalies (Förste *et al.* 2011) and geodetic data (Szeliga *et al.* 2012), and building on previous authors' examination of the geology, we first assess the kinematics of the range. We then discuss the evidence for determining the main factors governing the dynamics of the range, and present numerical models to provide insights into its deformation and evolution.

### 1.1 Tectonic setting

The western part of the Himalayan collision zone is comprised of a series of NNE–SSW left-lateral strike-slip faults (of which the well-known Chaman Fault is the westernmost), together with a ribbon of fold-thrust belts to the east (Fig. 1; Wellman 1966; Abdel-Gawad 1971; Lawrence & Yeats 1979; Farah *et al.* 1984; Stein *et al.* 2002; Szeliga *et al.* 2012). These fold-thrust belts divide Pakistan

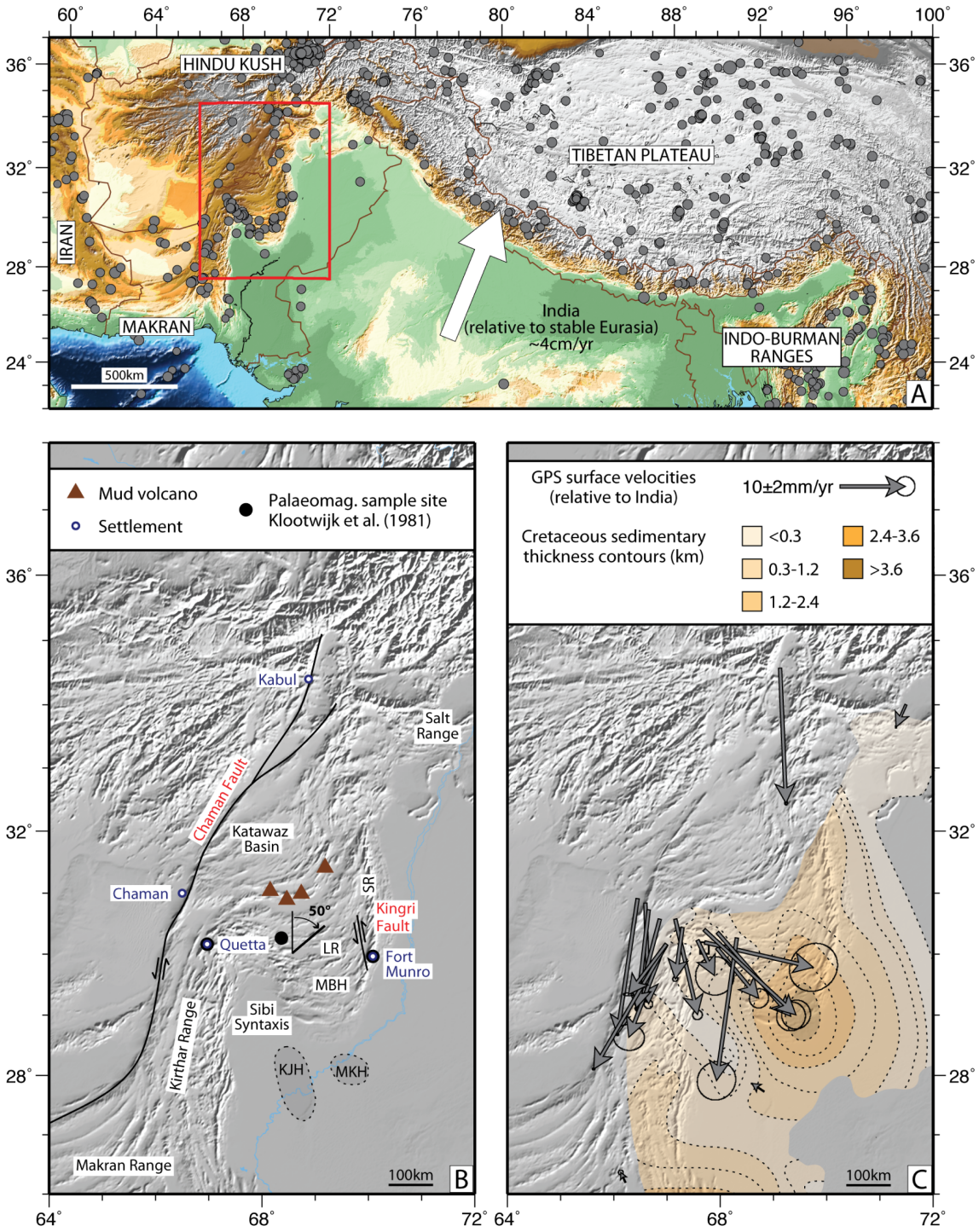


**Figure 1.** Geology and tectonic setting of the Sulaiman Range. (a) Regional setting. Brown lines are country boundaries; grey circles are $>M_w5.2$ earthquake locations from the EHB catalogue (Engdahl *et al.* 1998); white arrow is the MORVEL plate velocity vector of India relative to stable Eurasia (DeMets *et al.* 2010); red box shows the Sulaiman Range region shown in Fig. 3. (b) Overview map of the Sulaiman Range with mountainous regions commonly named in the literature (MBH – Mari Bugti Hills, LR – Loralai Range, SR – Sulaiman Range); tectonic features in black; faults named in red; and settlements in blue. Black dots are palaeomagnetic sample sites from Klootwijk *et al.* (1981), with rotation of sediments relative to Indian basement shown (if any). Dashed grey areas are Indian basement highs after Hunting Survey Corporation Ltd (1960), Auden (1974) and Humayon *et al.* (1991) and gravity data from Förste *et al.* (2011) (KJH – Khairpur-Jacobabad High, MKH – Mari-Kandikot High). (c) GPS surface velocities relative to India from Szeliga (2010) and Szeliga *et al.* (2012) and thickness contours of Cretaceous sediments from Kazmi & Rana (1982).

topographically and tectonically into a mountainous belt running from the Salt Range in the NE down to the Sulaiman and Kirthar Ranges in the SW, which sits beside the flat lowlands of the Indian Plate (Fig. 1). The strike-slip faults merge into the E–W folds and thrusts of the Makran convergence zone, where oceanic lithosphere of the Arabian Plate is being subducted beneath Afghanistan (considered to behave as part of Eurasia) (Jacob & Quittmeyer 1979; Lawrence *et al.* 1981; Treloar & Izatt 1993; Vernant *et al.* 2004);

and link it to the Himalayan convergence zone in the north, where Indian continental lithosphere is underthrusting Eurasia.

Unlike northern India, where the convergence direction is at a high angle to the plate boundary, the western boundary of the Indian Shield runs at a highly oblique angle to the predicted relative motion between India and Eurasia in this region (Fig. 1). This plate boundary must therefore accommodate a significant amount of left-lateral shear. The small convergent component of the relative motion, along with the buoyancy forces resulting from elevation contrasts (as discussed later), also leads to shortening along this margin. The result is a wide, transpressional plate boundary zone that generates diffuse seismicity from northeast Afghanistan to western Pakistan (Quittmeyer & Jacob 1979; Prevot *et al.* 1980), and which accommodates relative plate motion by a combination of strike-slip faulting in the Chaman fault system and thrust faulting in the fold belt to the southeast (Bernard *et al.* 2000; Szeliga *et al.* 2012). A component of the N–S convergence may also be taken up by left-lateral motion on strike-slip faults within the fold-thrust belt, such as the Kingri Fault (Rowlands 1978; Humayon *et al.* 1991; Bernard *et al.* 2000, Fig. 1b). As the Eurasian Plate margin and accompanying fold-thrust belts rotate from NNE–SSW in northern Pakistan to E–W in the Makran region, fault traces showing dominantly left-lateral motion curve to the southwest and may become active thrusts, or reactivate older structures in a strike-slip sense. This region produced the 2013 September 24 $M_w$7.7 strike-slip event (Avouac *et al.* 2014).

### 1.2 Previous work

Some previous attempts to explain the geometry, topography and tectonics of the Sulaiman Range have focussed on modelling the fold-thrust belt as a thin-skinned frictional wedge overlying the rigid, underthrusting Indian Plate (Humayon *et al.* 1991; Davis & Lillie 1994; Haq & Davis 1997; Macedo & Marshak 1999). Observations of surface geology and seismic reflection profiles from the eastern and southern range front indicate duplex-style thrusting under a passive roof thrust (Banks & Warburton 1986; Humayon *et al.* 1991; Jadoon *et al.* 1993). Using arguments from critical wedge theory (e.g. Davis & Engelder 1985; Dahlen 1990), the great across-strike width, flat top and gentle taper are taken as evidence for the presence of a weak basal decollement, thought to be provided by thin Eocambrian salt or evaporites, such as those seen in the Salt Range to the north (Sarwar & De Jong 1979; Banks & Warburton 1986; Humayon *et al.* 1991). Both Haq & Davis (1997) and Macedo & Marshak (1999) use sandbox models to investigate the development of the Sulaiman Range. Haq & Davis (1997) infer the presence of a fault-bounded rigid block at the western boundary of the Sulaiman Range, which is free to translate along the Chaman Fault and generate a variety of structures in the foreland basin sediments thrust against it. However, Macedo & Marshak (1999) suggest that the advancement of the Sulaiman Range is basin-controlled. They note that the apex of the lobe coincides with the depocentre of a package of Mesozoic sediments (Fig. 1c). Using critical taper theory, they argue that less internal deformation is needed to maintain a critical taper angle in the region of deeper sediment and so the fold-thrust wedge would be expected to advance more rapidly into this region. Humayon *et al.* (1991) and Davis & Lillie (1994) emphasize the great thickness of the stratigraphic sequence, postulating that because the range interior is made up of a very thick sedimentary sequence dominated by fine carbonate muds, conditions at the base will favour ductile deformation. They suggest that though the surface deformation is characterized by duplex thrusting, the lower portion of the sedimentary sequence deforms in a ductile manner, sliding over (and remaining mechanically coupled to) the Indian basement.

Bernard *et al.* (2000) used body waveform modelling to constrain the source parameters of 10 earthquakes that occurred between 1964 and 1985. They observed that the slip vectors of thrust events were approximately perpendicular to the local orientation of the range front, following the curvature of the lobe. They produced a model of the region subject to both the relative motion between India and Afghanistan and gravitational driving forces, with an imposed weak zone representing the Chaman Fault. They did not include the Indian basement underthrusting the range.

We build upon these previous studies by obtaining well-constrained focal parameters for additional earthquakes, and by constructing a dynamic model to investigate the major controls on the deformation and evolution of the topography. We use the combination of new focal mechanisms and our dynamic models to identify the most important factors governing the dynamics of the range, and distinguish between the hypotheses put forward by other authors. Our models and results shed new light on the factors controlling the behaviour of this mountain range, and are applicable to fold-thrust belts in general.

## 2 GEOLOGICAL SETTING

The Sulaiman Range (in this paper taken to mean the whole lobate fold thrust belt, including the Sulaiman Range in the east, the interior Loralai Range and the southern Mari-Bugti Hills, Fig. 1b) is the widest of the Pakistani fold-thrust belts (Fig. 1b). It is composed of a passive margin sequence of Mesozoic platform carbonates, sands, muds, shales and volcanics which show a deep-water affinity to the north. These deposits transition to younger siliciclastic sediments shed from the newly forming Himalaya from the Eocene onwards and deposited in a shallow-water deltaic environment analogous to the modern-day Indus delta-fan system (Eames 1951; Humayon *et al.* 1991; Treloar & Izatt 1993; Qayyum *et al.* 1996, 2001; Kassi *et al.* 2009). The sedimentary sequence was deposited in a large basin off the western Indo-Pakistani subcontinent; the southwestern continuation of the remnant Neo-Tethys Ocean being consumed to the north throughout the early Cenozoic (Qayyum *et al.* 1997). Just east of the Chaman fault this sequence is known as the Katawaz Basin sequence. The same time-transgressive clastic sequence extends into the Sulaiman foredeep (Treloar & Izatt 1993) and is topped by younger Himalayan molasse. The Sulaiman Range is therefore the uplifted and deformed passive margin sequence of the northwestern edge of the Indian Plate, now accreted to eastern edge of the Afghan Block and being underthrust by the Indian Plate.

Seismic profiles and borehole data indicate that the cover sequence (in this paper taken to mean all sediments of Mesozoic age and younger, sitting atop crystalline basement) is >8 km thick at the eastern range front, and thickens to the northwest to ~14 km at the Kingri Fault (Fig. 1b) and over 20 km in the range interior, due to tectonic shortening (Banks & Warburton 1986; Humayon *et al.* 1991). Seismic reflection profiles indicate that the depth to basement increases to the NW (Humayon *et al.* 1991). This, taken together with the large stratigraphic thickness of platform sediments and the presence of ophiolite bodies thrust on top of this sequence in the range interior (Hunting Survey Corporation Ltd 1960), suggests that the Sulaiman Range may be underlain by thinned passive margin, not full thickness continental crust. Shear wave velocity

models produced from surface wave data give higher than expected velocities for the lower crust in this region, suggesting that transitional to oceanic crust may underlie parts of the Sulaiman Range (Chun 1986).

### 2.1 Shortening

Though there has been significant uplift in the Sulaiman Range—Auden (1974) notes that Jurassic limestones have been uplifted over 6 km above the regional level—it is not clear how much shortening has occurred. Jadoon (1991), Humayon *et al.* (1991) and Banks & Warburton (1986) all estimate as much as 50–60 per cent shortening of the sedimentary sequence, based on seismic reflection data and palinspastic restoration. This approach has a number of caveats: (1) The curved morphology of the anticlinal ridges (concealing buried thrusts) suggests that the path material follows towards the margins of the fold-thrust belt is curved; i.e. the cross-sections are oblique to the transport direction. (2) The seismic reflection data only cover a small portion of the cross-sections—the frontal folds of the southern and eastern range fronts—and they do not penetrate deep enough to image the basement. (3) Due to a lack of stratigraphic constraints in the range interior, no allowance has been made for thickening of the sedimentary units; however, from the direction of collision we might expect that the basin in which the cover sequence was deposited may have deepened towards the west. (4) Estimating shortening by restoring cross-sections implicitly assumes the deformation is brittle, however Jadoon (1991) postulates that the cores of the frontal anticlines have been filled by ductile flow of fine-grained carbonates; a mechanism that is likely to operate on a larger scale at depth in the range interior, where the stratigraphic sequence is much thicker and therefore the temperatures hotter (Davis & Lillie 1994).

## 3 TOPOGRAPHY AND GRAVITY ANOMALIES

The Sulaiman Range is conspicuous due its extensive width (~500 km) compared to its along-strike length (~300 km), and its extreme plan-view curvature. In contrast to the narrow ranges on either side, it forms a large, asymmetric, flat-topped lobe, slightly inclined to the southeast, with an average elevation of 2 km (Fig. 1). Steep range fronts mark the east and west sides, similar to those along the margins of the Kirthar Range to the south, and in contrast to the gentle, southerly dipping apex (Fig. 2). Discontinuous, arcuate, anticlinal ridges mark the trend of 10–20-km-wavelength surface folding, which form curved lines in plan view and converge at the endpoints of the lobe (Fig. 1b). Many of the frontal folds conceal blind thrusts, the majority of which verge towards the Indian foreland (Banks & Warburton 1986; Bernard *et al.* 2000). En echelon anticlinal folding along the linear eastern range front is likely to accommodate N–S left-lateral shear between the Sulaiman Range and the narrow highlands to the NNE via oblique thrusting. This style of accommodation is less developed on the western range front, which forms the eastern border of the Sibi Syntaxis (Fig. 1b). No thrust faulting has been recognized in the folded Katawaz Basin sediments in the interior of the Sulaiman Range (Lawrence *et al.* 1981).

Flexure due to topographic loading produces long-wavelength asymmetric signals in the free air gravity anomaly on the margins of the range (Fig. 2). The absence of a large negative anomaly adjacent to the nose of the range implies less loading of the Indian lithosphere than elsewhere along the range front, suggesting a thinner sedimentary load than elsewhere in the Sulaiman Range (and the Pakistan fold belts in general). The ~150 km wavelength of the gravity anomalies on the margins of the range indicates an elastic thickness of >~30 km, as is also seen where India underthrusts the

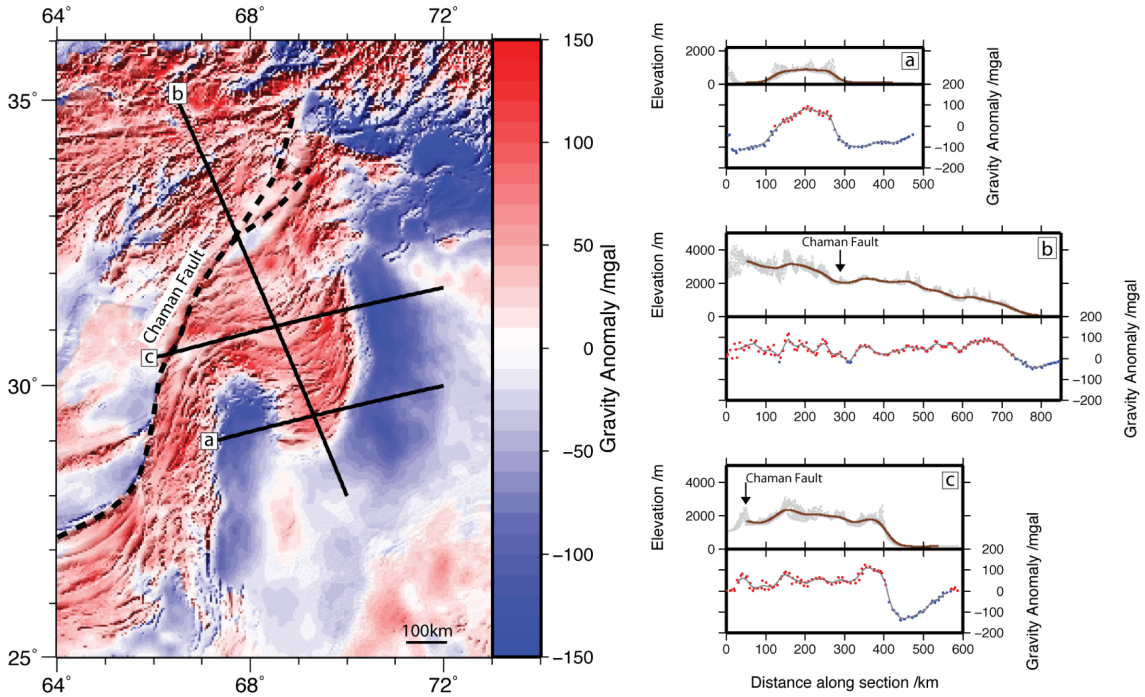


**Figure 2.** Topography and gravity anomaly of the Sulaiman Range. Map shows SRTM30 topography overlain with EIGEN6C free-air gravity anomaly (Förste *et al.* 2011). This gravity model has a degree and order of 1440, which can resolve features with a ≥14 km half wavelength (Förste *et al.* 2013). Red is a positive gravity anomaly, blue negative. Profiles a–c show filtered long-wavelength (100 km Gaussian filter) topography (upper panel) and gravity anomaly (lower panel) along section.

Himalaya (Jackson *et al.* 2008). Sparse seismicity within northern India extends to depths of ∼45 km (Craig *et al.* 2012). Taken together, these results imply that the Indian lithosphere is cool and strong (e.g. Jackson *et al.* 2008).

## 4 ACTIVE DEFORMATION

### 4.1 GPS

The geodetic data available for the Sulaiman Range is very limited, with no coverage in the centre of the range (Fig. 1c). Velocities near the Chaman fault represent a combination of the motion of Afghanistan relative to India and the interseismic strain accumulation around the N–S-striking left-lateral strike-slip faults. Estimated velocities further east, within the SW section of the Sulaiman lobe, show the roughly southeastwards motion of the range interior towards the interior of the Indian Plate (at ∼10–20 mm yr$^{-1}$).

### 4.2 Seismicity

#### *4.2.1 Previous work*

Instrumental and historical evidence shows that the Sulaiman Range and surrounding area exhibits a high level of seismic activity, though events with a magnitude $\geq M_w6$ are infrequent and only three $\geq M_w7$ events have occurred in the last century (Fig. 3). As the Sulaiman Range is a remote and sparsely populated mountainous desert, it is not unexpected that there is very little documented evidence of earthquakes prior to the late 19th century (Ambraseys & Bilham 2003b). We briefly describe some of the significant events in the Sulaiman Range region, summarized from Ambraseys & Bilham (2003b).

The first significant earthquake to be described in detail in this region was the 1892 December 20 Chaman earthquake (Griesbach 1893), after which the Chaman Fault is named. Anecdotal evidence suggests the Chaman Fault has produced surface-rupturing earthquakes prior to this (Quittmeyer & Jacob 1979; Armbruster *et al.* 1980). Observations of offset railway lines and surface fissuring near the town of Chaman, on the Pakistan–Afghanistan border, show that this was a left-lateral strike slip event with a component of vertical motion (Griesbach 1893; Quittmeyer & Jacob 1979; Armbruster *et al.* 1980; Ambraseys & Bilham 2003b). Surface observations at the time indicate that the fault ruptured along a 16–32 km segment (Griesbach 1893; Ambraseys & Bilham 2003b).

No large ($\geq M_w6$) earthquakes have occurred on the Chaman Fault during the instrumental period. Five moderate events occurring between 1974 and 1978 had mechanisms consistent with left lateral motion on a NNE–SSW striking fault (blue mechanisms on Fig. 3a), and two of these (from 1975) are known to have ruptured the surface (Jackson & McKenzie 1984). GPS velocities indicate that at least part of the fault has a shallow locking depth of ∼3 km and a slip rate of 8–17 mm yr$^{-1}$ (Szeliga *et al.* 2012), however there are no well-constrained earthquake centroid depths for events occurring on the Chaman Fault.

Three significant earthquakes occurred in the northern Kirthar Range and Sibi Syntaxis area, contiguous in both space and time; the 1931 $M_w6.8$ Sharigh, 1931 $M_w7.3$ Mach and 1935 $M_w7.7$ Quetta earthquakes (Szeliga *et al.* 2009) (solid yellow circles on Fig. 3a). The mechanism of the 1931 Sharigh event is not known (Quittmeyer & Jacob 1979). Remeasurement of a levelling line, together with structural interpretation of seismic reflection data suggests the Mach earthquake was a thrust event that ruptured a W-dipping, blind ramp-and-flat system on the eastern range front of the northern Kirthar Range (Bannert 1992; Szeliga *et al.* 2009). The 1935 Quetta earthquake was a surface-rupturing left-lateral strike-slip event (Quittmeyer & Jacob 1979; Armbruster *et al.* 1980) that occurred on a fault parallel to the Mach event and ∼100 km west of it (Ambraseys & Bilham 2003b). This is a structurally complex region, where the NNE–SSW trending Kirthar Range meets the NW–SE thrusts of the western Sulaiman Range (Fig. 1b), and which has also seen several recent damaging earthquakes. A $M_w6.9$ and $M_w6.7$ double event occurred in the Sibi Syntaxis area on 1997 February 27 (orange mechanisms on Fig. 3). Analysis of InSAR interferograms and elastic dislocation modelling has revealed coseismic slip on two buried thrust faults; the NW fault rupturing between depths of 10 and 20 km and showing no link between coseismic uplift and surface topography, the SE showing slip up to ∼4 km depth and coseismic uplift along an anticline (Nissen *et al.* 2011a). A pair of $M_w6.4$ strike-slip earthquakes also occurred NE of Quetta on 2008 October 28 and 29 and were followed by a sequence that culminated in a $M_w5.7$ aftershock on 2008 December 9. The region of this seismic sequence has been the subject of several differing studies. An early LandSat imagery study by Kazmi (1979) postulated the existence of extensive NNW–SSE basement lineaments running through the area, underneath the cover sequence. MonaLisa & Jan (2010) and Yadav *et al.* (2012) suggest slip occurred on one or more faults parallel to this trend, on the basis of seismological studies. Using GPS data, Khan *et al.* (2008) also inferred slip on NW–SE orientated faults at depths around the expected basement–cover interface, though it is not known whether the faulting ruptured the basement, cover or both. Conversely, Szeliga (2010) used a combination of teleseismic waveform data and InSAR data to model the source parameters and proposed a bookshelf-faulting model, with clockwise rotation of blocks bounded by parallel NE–SW left-lateral strike-slip faults. More recently, both Pezzo *et al.* (2014) and Pinel-Puysségur *et al.* (2014) inverted InSAR data to model the source parameters and slip distributions for these events, and proposed a combination of right-lateral motion on large NW–SE fault planes, bounding a region of clockwise-rotating blocks with left-lateral motion on smaller NE–SW faults. Aside from some N–S trending fissures, no surface rupture was observed in this region (Szeliga 2010), and the trend of pre-existing surface folding is at odds with the orientation of the proposed fault geometries. This suggests that surface folding is decoupled from faulting deeper in the sedimentary sequence, or that the deformation style has evolved through time. Despite the controversy over the kinematics in this area, it is clear that it accommodates significant right-lateral shear between the Sulaiman Range and the Kirthar Ranges.

#### *4.2.2 New waveform-modelling results*

Building on the work of Bernard *et al.* (2000), we carried out teleseismic waveform inversion for 10 moderate-sized ($M_w \geq 5.2$) earthquakes from 1995 to 2008, that have not previously been analysed in detail. The Global Digital Seismogram Network (GDSN) broadband seismograms were filtered at 15–100 s to remove the high frequency part of the record, which is sensitive to source complexity and local variations in velocity structure, leaving only the long-period signal in which the earthquake approximates a point source. The events could then be modelled as point sources using the MT5 algorithm of McCaffrey *et al.* (1991) and Zwick *et al.* (1994), which simultaneously inverts *P* and *SH* waveform data for

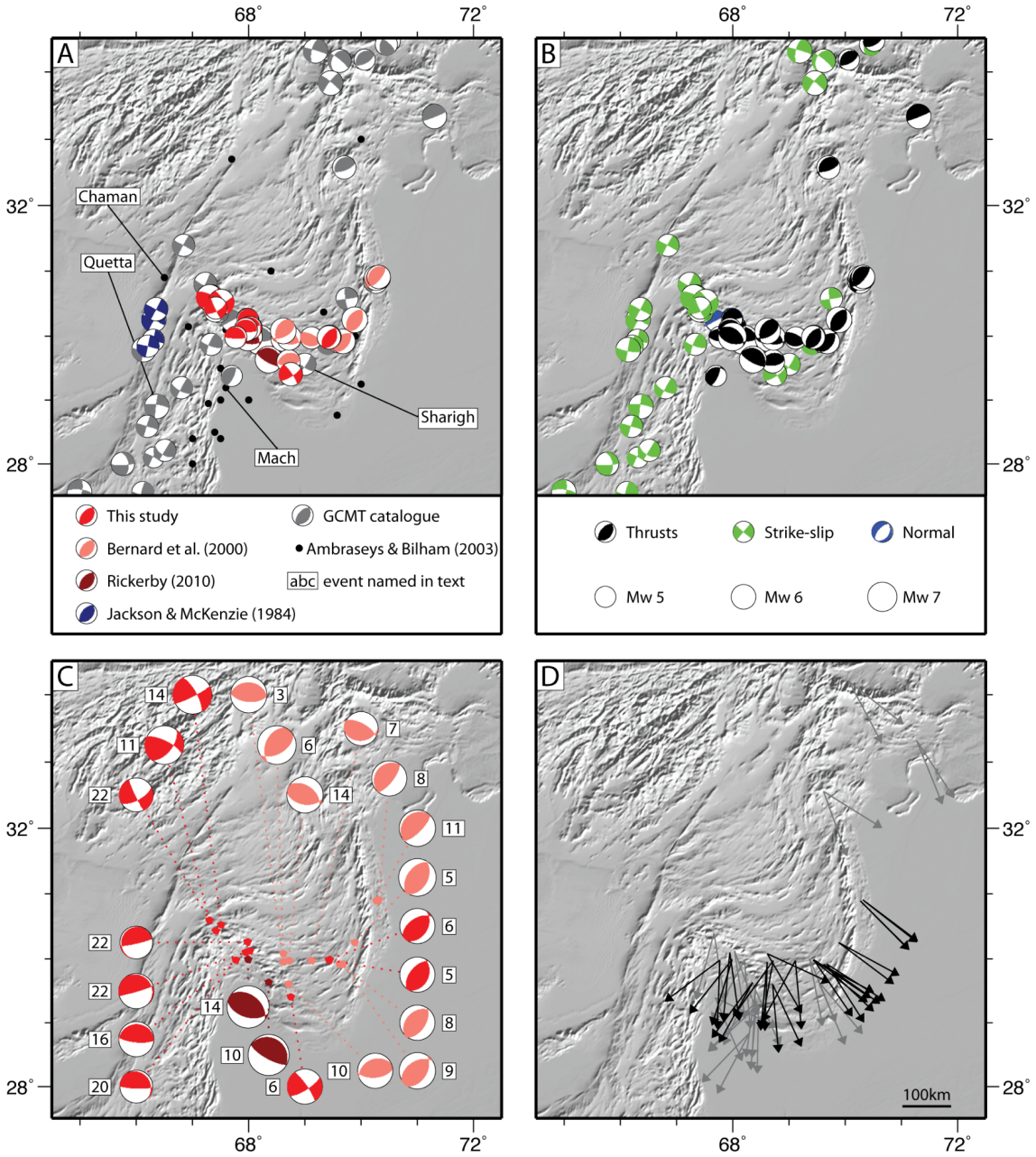


**Figure 3.** Seismicity of the Sulaiman Range. Events with magnitudes $\geq M_w 5.2$ shown. Events from the Global CMT catalogue occurring prior to 2010 are shown at the relocated EHB epicentres. (a) Focal mechanisms coloured by author and scaled according to magnitude. Epicentral locations shown for historical events from Ambraseys & Bilham (2003b). (b) Focal mechanisms coloured by rake. (c) Focal mechanisms and centroid depths constrained by body waveform inversion. Coloured as for (a). (d) Thrust slip vectors. Horizontal component of motion plotted for both nodal planes, showing motion of NW side relative to SE side (grey – GCMT focal planes solutions, black – mechanisms constrained by body waveform inversion).

source time function, strike, dip, rake, moment and centroid depth. This method generates synthetic seismograms and solves iteratively for the source parameters that give a minimum misfit between the observed waveform and synthetics within the inversion window. A full description of this routine method can be found in Taymaz *et al.* (1991) and Nábělek (1984). This technique refines the accuracy of source parameter estimates made by routine catalogues such as the GCMT, particularly for the centroid depth. Typical errors are ±4 km for depth, ±10° for strike, ±5° for dip and ±10° for rake (Molnar & Lyon-Caen 1989; Taymaz *et al.* 1991). Sensitivity is determined by fixing a parameter, for example depth, at a range of values and letting all other parameters vary during multiple inversions. The fit of the synthetic to the observed seismograms is then compared at successive values of the fixed parameter to determine the range over which a reasonable fit has been found. Fig. 4 shows an example result for body waveform inversion of an event that occurred on 1997 March 20.

The minimum misfit solutions of the earthquakes we have studied are shown in Table 1, full waveform inversion results are shown in Appendix A, and focal mechanisms are plotted on Fig. 3 [along with those of the 10 events from 1966 to 1985 modelled by Bernard *et al.* (2000); the double event from 1997 modelled by Rickerby (2010); 26 events from the Global Centroid Moment Tensor catalogue; first motion solutions from Jackson & McKenzie (1984) and the

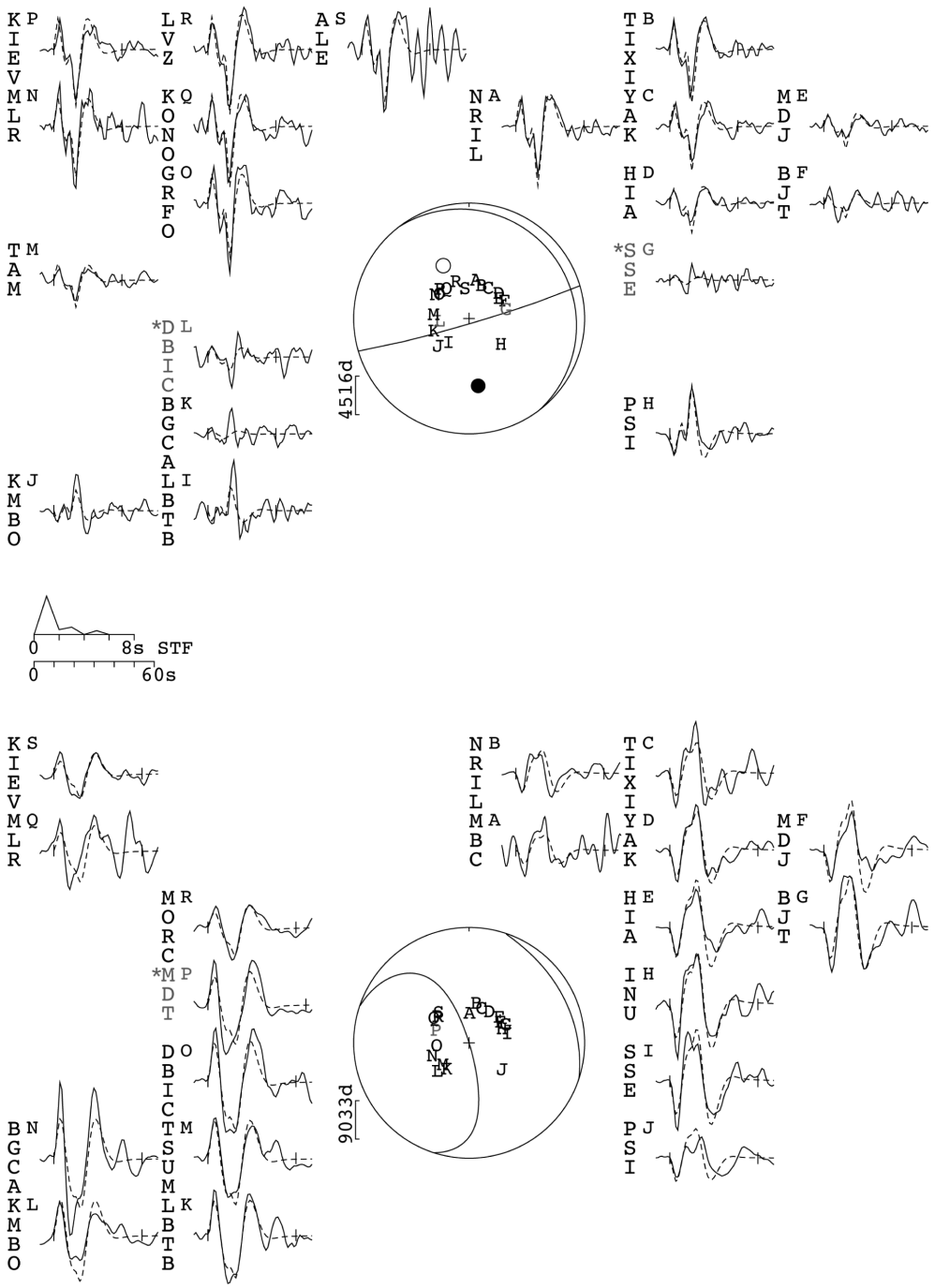


**Figure 4.** Body waveform inversion results for a $M_w$5.6 event that occurred near Harnai, on 1997 March 20. The upper panel shows all seismograms inverted for *P* waveforms, the lower those for SH waveforms. The title gives the date (yyyy-mm-dd) and moment magnitude of the event; the subtitle gives the focal mechanism parameters (strike/dip/rake/centroid depth/scalar moment) obtained via the inversion. Seismograms are labelled with the station name (e.g. NRIL) and alphabetic tag (e.g. A), assigned (in alphabetical order) according to azimuth, clockwise from north. Seismograms are plotted around the appropriate lower hemisphere projections of the focal sphere (*P* or *SH*) at their approximate station azimuth and the tag is plotted on the lower hemisphere projection at the point of intersection of the ray path. Observed seismograms are plotted with a solid line, synthetics with a dashed line, and the ticks mark the window of data used in the inversion. Black and white circles show the *P*- and *T*-axes, respectively. The amplitude scale (micrometres) is given to the bottom left of the focal sphere (N.B. for visual clarity, this may differ for *P* and *SH* waveforms). The source–time function (STF) is plotted under the *P* hemisphere, the seismogram timescale below.

**Table 1.** Teleseismic body waveform modelling results.

| YYYY | MMM | DD | Lat (°) | Long (°) | Strike 1 | Dip 1 | Rake 1 | Strike 2 | Dip 2 | Rake 2 | Depth (km) | $M_0$ (Nm) | $M_w$ |
|---|---|---|---|---|---|---|---|---|---|---|---|---|---|
| 1995 | May | 31 | 30.257 | 67.984 | 077 | 85 | 99 | 196 | 10 | 29 | 22 | $8.5 \times 10^{16}$ | 5.2 |
| 1997 | Mar | 4 | 29.405 | 68.748 | 058 | 74 | 11 | 325 | 79 | 164 | 6 | $4.6 \times 10^{17}$ | 5.7 |
| 1997 | Mar | 20 | 30.125 | 68.022 | 322 | 10 | 158 | 074 | 86 | 81 | 22 | $3.1 \times 10^{17}$ | 5.6 |
| 1997 | Aug | 24 | 30.100 | 67.944 | 262 | 16 | 77 | 096 | 74 | 94 | 16 | $2.9 \times 10^{17}$ | 5.6 |
| 1997 | Sep | 7 | 29.981 | 67.768 | 323 | 14 | 140 | 092 | 81 | 79 | 20 | $9.9 \times 10^{16}$ | 5.3 |
| 1999 | Jun | 26 | 29.991 | 69.436 | 034 | 40 | 73 | 236 | 52 | 104 | 6 | $2.8 \times 10^{17}$ | 5.6 |
| 1999 | Jul | 12 | 29.979 | 69.432 | 028 | 35 | 82 | 218 | 55 | 96 | 5 | $3.7 \times 10^{17}$ | 5.6 |
| 2008 | Oct | 28 | 30.597 | 67.299 | 296 | 71 | 145 | 039 | 57 | 23 | 11 | $4.2 \times 10^{18}$ | 6.3 |
| 2008 | Oct | 29 | 30.518 | 67.515 | 331 | 72 | 172 | 064 | 82 | 18 | 14 | $3.2 \times 10^{18}$ | 6.3 |
| 2008 | Dec | 9 | 30.433 | 67.414 | 062 | 65 | −5 | 154 | 85 | −155 | 22 | $2.3 \times 10^{17}$ | 5.5 |

locations of pre-instrumental earthquakes from Ambraseys & Bilham (2003b)].

Considering our earthquake source inversion results, along with previous studies, the seismicity of central Pakistan can be summarized as follows.

High-angle reverse faulting occurs in an arcuate band across the nose of the Sulaiman lobe (Fig. 3b). The earthquakes occur close to the steep topographic front on the east and west sides of the lobe, but are spread over, and set back from, the end of the gently inclined nose. Modelled fault plane strikes follow the shape of the lobe and the strikes of arcuate surface folds, so that slip vectors fan out around the range front, but are slightly oblique to its strike (Fig. 3d), indicating that the thrust transport direction is obliquely radial to the range front. The close association of thrust-fault orientation with range-front geometry indicates that the thrusting may be driven by topographic contrasts, as discussed below. Well-constrained centroid depths are shallower than 11 km in this band (Fig. 3c). The average magnitude is $\sim M_w 5.5$, which corresponds to rupture on a $\sim 5 \times 5$ km fault plane, assuming a displacement-length ratio of $5 \times 10^{-5}$ (Scholz 1982). Given that the sedimentary pile is >8 km thick at the range front, and deepens to the NW to over 20 km (Banks & Warburton 1986; Humayon *et al.* 1991; Jadoon *et al.* 1993), and that these thrust faults have centroid depths dominantly in the range 5–10 km, it is likely that the seismicity is contained wholly within the cover sequence; i.e. that the Indian continental basement is not involved. Some deeper, low-angle thrust events occurring in the Sibi Syntaxis region have modelled centroid depths in the range of 16–22 km—depths approaching the expected interface between the sedimentary pile and Indian basement. Unlike the thrusting in the rest of the Sulaiman lobe, these events had one nodal plane dipping at <30°, suggesting that they may give the dip and depth of the cover–basement interface.

There are a number of strike-slip events located within the Sulaiman lobe, in the same area as the thrust faulting (Fig. 3), that can be grouped as follows: (1) events occurring near the nose of the range, which have N–S *P*-axes and E–W *T*-axes. (2) Events occurring in the east of the range, which are located along or near a mapped strike-slip fault, the Kingri Fault (Fig. 1b). (3) A group of three events from an earthquake and aftershock sequence that occurred near Quetta in 2008. For these three events we obtained best-fitting mechanisms with strike-slip to oblique thrust motion on high-angle fault planes, in good agreement with those obtained by Szeliga (2010) (discussed above). Our centroid depths are in the range 11–22 km, which is deeper than those for strike-slip events elsewhere in the Sulaiman Lobe.

No significant seismicity has been observed during the instrumental period in the interior plateau-like region of the Sulaiman Range. For the section of the Chaman Fault between 31°N and 34°N there is no documented evidence of a significant earthquake (Ambraseys & Bilham 2003a). Comparison of moment release calculations for the last century and strain rate and velocity field models indicates that there is a large seismic moment deficit in the Sulaiman Range, and along this section of the Chaman Fault in particular (Bernard *et al.* 2000; Ambraseys & Bilham 2003b). This deficit may be due in part to our short period of observation, but also raises the possibility that strain may be accommodated by ductile mechanisms within the carbonate- and mud-rich sedimentary pile making up the Sulaiman Range.

## 5 DYNAMIC MODELLING

This section describes numerical models that have been produced in order to provide insights into the forces and rheology generating the observed topography and deformation of the Sulaiman Range. We designed models in order to investigate the dynamic controls on the long-wavelength (≥100 km) topography and deformation in this region; they are not intended to replicate the exact geometry of individual anticlines or faults, but the first-order characteristics of the entire region.

### 5.1 Model rheology and dynamics

The lateral change in topography from elevated mountain to low-lying plains results in a horizontal gradient in gravitational potential energy. This gradient results in a horizontal force that acts to minimize the difference in potential energy by reducing the elevation contrast between highland and lowland by thinning the mountains and thickening the lowlands. This force will act parallel to topographic gradients. In contrast, the relative motion between bounding plates will result in a force with the same orientation throughout a collision zone. The rapid along-strike variations in shortening direction (fanning thrust slip vectors in Fig. 3d) in the Sulaiman Range, which largely mirror the changing strike of the range, imply that gravitational forces acting on topographic contrasts play an important role in the behaviour of this region.

We chose to use the simplest model setup that includes the physics required to match our observations of the Sulaiman Range. We follow previous authors in exploring the dynamics of mountain ranges by approximating their behaviour as that of a viscous fluid (e.g. England & McKenzie 1982; Houseman & England 1986; Royden 1996; Flesch *et al.* 2001; Bendick *et al.* 2008). For the rheology of the Sulaiman Range we use a constant-viscosity Newtonian fluid.

This type of model implicitly assumes that the behaviour of the deforming region is continuous. The interior of the Sulaiman Range (the plateau-like area NW of the seismically active band along

the range front) is largely aseismic, and is made up of a ~20 km sequence of fine grained carbonates and shales. Ductile deformation mechanisms (e.g. pressure-solution or diffusion creep) are likely to operate, particularly towards the bottom of the thick sedimentary pile. These mechanisms are known to occur in shale and carbonate sediments at relatively low temperatures (as low as ~200 °C) (Rutter 1983), and will result in a Newtonian viscous rheology. This style of deformation has been suggested both for the Sulaiman Range (Davis & Lillie 1994) and geologically similar regions, such as the Indo-Burman Ranges (Copley & McKenzie 2007). Examples of ductile deformation have been observed in shales and carbonates exposed in the cores of folds in the hinterland of the Sulaiman Range, and is inferred from seismic lines to occur in the cores of the frontal anticlines (Jadoon *et al.* 1993). Combined with the regional seismic moment deficit (Bernard *et al.* 2000; Ambraseys & Bilham 2003b), it is likely that aseismic, ductile processes are important in the Sulaiman Range. We therefore assume a Newtonian fluid rheology. For simplicity, we use a constant viscosity in our model; this is a representation of the average mechanical properties of the Sulaiman Range. We discuss later the effects of using a more complex rheology.

The Indian Plate is thought to maintain its strength along its margins, where it is underthrusting the Tibetan Plateau and Indo-Burman Ranges (e.g. Nábělek *et al.* 2009; Copley *et al.* 2011). Thermal modelling of the Indian Shield suggests that the Indian lower crust is slow to heat up as it underthrusts Tibet, retaining its strength and acting as a rigid base to the warmer material above (Craig *et al.* 2012). Therefore we follow Copley (2012) in modelling the Sulaiman Range as a viscous fluid over-riding a rigid base. These conditions are equivalent to the 'Type 3' model of Bendick & Flesch (2013), where the dominant style of deformation is the shearing of a weak layer over a stronger substrate. Bernard *et al.* (2000) investigated the dynamics of the Sulaiman Range using a 'Thin-Viscous-Sheet' numerical model. That type of model assumes that there are negligible shear stresses exerted on the base of the deforming layer, and therefore that there are no vertical gradients of horizontal velocity (i.e. no underthrusting). Our model differs from theirs because we model the Indian Shield as a rigid base to the Sulaiman Range, which exerts shear stresses upon the base of the deforming layer.

Well-established fluid-dynamic theory shows that topographically induced pressure gradients will cause a pile of viscous fluid on a rigid base to flow outwards and form a circle in plan view, with a flat top, steep sides and radial horizontal surface velocity vectors (e.g. Huppert 1982). This simple picture does not explain all the features we observe in the Sulaiman Range—the range front does not form a perfect arc but an elongate lobe, and the thrust slip vectors are slightly oblique to the range-front curvature. The high degree of curvature, strong asymmetry, the gentle gradient down the nose (compared to the steep east and west topographic fronts), and the oblique transport direction observed in the Sulaiman Range suggest that some additional factor is controlling the evolution of the range. In this section, we investigate what could lead to the lateral variations in topographic slope and the extensive across-strike width of the Sulaiman Range compared to adjacent ranges.

Changing the boundary conditions on the base of a flowing layer, for example, the degree of coupling to an underlying substrate, will change the characteristics of the deformation and the resulting topography (e.g. Ellis 1996). Reducing the degree of coupling to the substrate will result in a gentler surface gradient and higher surface velocities (McKenzie *et al.* 2000). The Sulaiman Range has propagated much further over the Indian foreland than adjacent fold-thrust belts, though they have presumably been extant for approximately the same length of time. It also has a gentle topographic slope down the apex of the lobe (Fig. 2, profile b), in stark comparison to the steep-fronted Kirthar Range to the south. This suggests that the Sulaiman Range has a lower degree of basal coupling to the underthrust Indian lithosphere than the fold-thrust belts either side.

Kazmi & Rana (1982) show Cretaceous sedimentary isopach contours on their geological map of Pakistan (Fig. 1c), revealing a pre-existing basin on the Indian plate, adjacent to the Sulaiman Range, with a depocentre that coincides with the apex of the range. It is likely that this depocentre contains weak sedimentary horizons which could act as detachment horizons. The exact nature of these units is not known. Sarwar & De Jong (1979) and Banks & Warburton (1986) suggested the presence of thin Eocambrian salt or evaporites, such as those seen in the Salt Range to the north. Although salt has been found in a well 200 km east of the Sulaiman range front, it is not observed in seismic profiles across the range front (Humayon *et al.* 1991) nor is there any surface evidence of salt tectonics. However there are a number of active mud volcanoes scattered across the Sulaiman Range (Hunting Survey Corporation Ltd 1960), indicating the presence of overpressured shales within the sedimentary sequence (Fig. 1b). These would also act as weak decoupling horizons.

In our model we will examine the effects of lateral variations in mechanical coupling (due to weak horizons contained within the pre-existing Mesozoic basin) on the tectonics of the range. Macedo & Marshak (1999) first suggested that the tectonics of the Sulaiman Range were basin-controlled, though as a result of varying sediment thicknesses, not sediment rheology. Other authors (e.g. Sarwar & De Jong 1979; Banks & Warburton 1986) have previously suggested the tectonics are influenced by the presence of weaker sedimentary horizons. We build upon their work by constructing a numerical model to test the dynamic implications of an advancing fold-thrust belt interacting with a pre-existing basin containing weak sediments.

### 5.2 Model setup

For simplicity, we model the Sulaiman Range as a Newtonian viscous fluid with a constant viscosity. Using the method of Copley (2008), the equations for fluid flow in the absence of inertial forces are solved in three dimensions. Velocity fields are calculated using the finite difference method. The driving forces are the imposed boundary conditions (described below), and gravity acting on topographic contrasts. Time-stepping is achieved by rewriting the incompressibility condition as a diffusion equation (Pattyn 2003), which is then solved using a Crank–Nicolson joint implicit–explicit scheme (Press *et al.* 2007).

We assume a constant viscosity for the entire layer, of $10^{20}$ Pa s. This is in the range of the viscosity Copley & McKenzie (2007) found for the Indo-Burman Range, $10^{19}$–$10^{20}$ Pa s, which is a lithologically similar fold-thrust belt in an analogous setting on the eastern margin of the Indian Plate. The rate of propagation of the model mountain range, but not the resulting patterns of topography and deformation, depend upon the choice of the viscosity, and we will discuss later the effects of choosing different values.

The model domain consists of a viscous layer, which has a rigid and deformable lower boundary (meaning the horizontal velocity is constrained to zero, but vertical motions can occur in order for the model topography to be isostatically compensated McKenzie *et al.* 2000) (Fig. 5). This boundary condition represents the rigid underlying Indian lithosphere and is equivalent to that used by

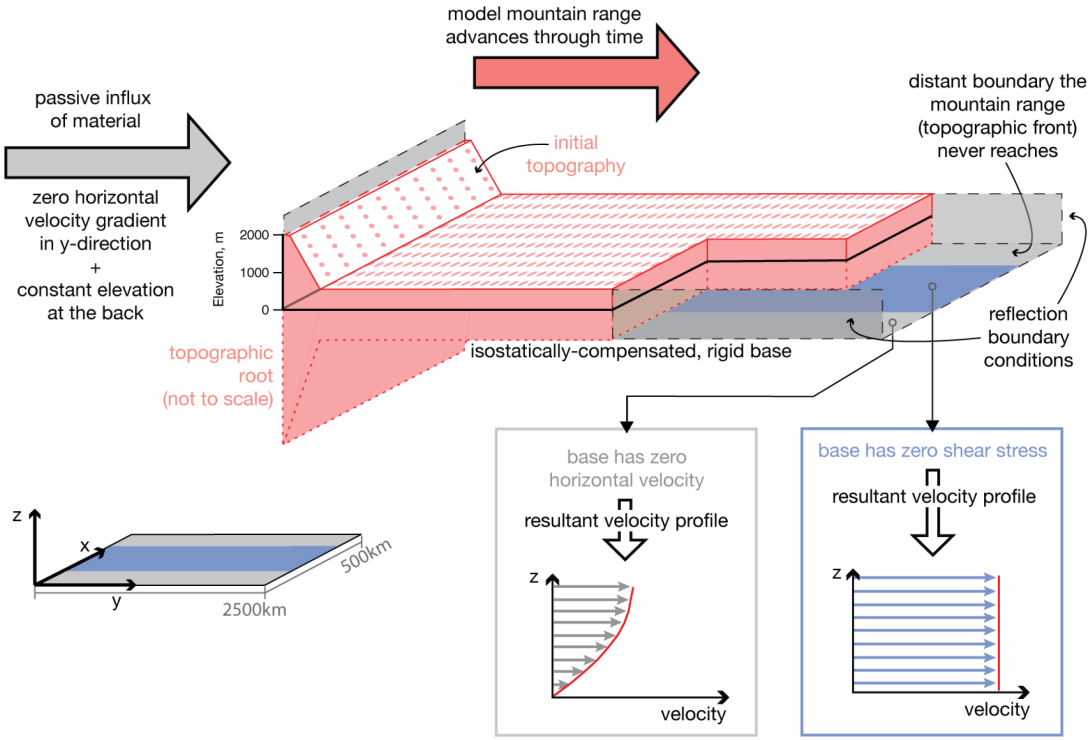


**Figure 5.** Initial numerical model setup and boundary conditions. Lower right insets show resultant velocity–depth profiles through the model viscous fluid. Lower left inset shows orientation of *x*-, *y*- and *z*-axes and dimensions of the model domain.

Bendick *et al.* (2008) and Copley & McKenzie (2007) to model the area of the Tibetan Plateau that overlies the underthrusting Indian lithosphere. Our assumption of isostatic equilibrium neglects the flexural strength of the underthrusting Indian lithosphere. However, such an assumption has a minimal effect on the applicability of our model results. McKenzie *et al.* (2000) compared the behaviour of a thin fluid layer flowing over a rigid, isostatically compensated base with one flowing over a horizontal base (which is equivalent to the end-member situation in which the Indian lithosphere has a high enough elastic strength that it is undeformed by the load of the overthrust mountain ranges). They found that the behaviour of the currents was the same, with the exception that the isostatically compensated current flowed more rapidly, by a scalar factor related to the thickness of the compensating root. As described below, the age and rates of motion in the Sulaiman Ranges are relatively poorly known, and are not used in assessing the results of our models. Instead we focus on the shape of the topography and the location and orientation of active deformation. These features of the model results are not affected by whether or not the range is isostatically compensated.

We impose an initial topography along one end of the model—a thin, linear mountain range with triangular cross-section—such that the $y = 0$ boundary has a constant elevation of 2000 m. As our model range is isostatically compensated, this surface elevation corresponds to a layer thickness of 20 km, which is similar to estimates of the depth to the basement under the Katawaz basin (Banks & Warburton 1986; Humayon *et al.* 1991). This material represents the thickened and uplifted strata of the passive continental margin that now forms the Pakistani fold-thrust belts. Elsewhere, the viscous layer is thin, with a flat topography, representing the sediments overlying the Indian Plate distant from the Sulaiman Range. Provided this layer thickness is small compared with the elevation of the range, it has little influence on the model behaviour (McKenzie *et al.* 2000).

Along the $y = 0$ boundary (Fig. 5) we impose a zero horizontal velocity gradient in the *y*-direction (on both horizontal components of the velocity), which assumes that material from an unseen reservoir can be drawn in passively behind the advancing model mountain range (Copley 2012). This condition is equivalent to there being a reservoir of crust that can be drawn into the Sulaiman Range (i.e. the thickened continental margin sediments in the region of the Katawaz Basin, and the highlands of north Afghanistan). The range propagates across the model domain due to gravity acting on the elevation contrasts. At very high values of y (distant enough that the propagating flow does not interact with them) we impose rigid boundary conditions (i.e. the horizontal velocity is zero). At the lateral edges of the model domain (in the *x*-direction) we impose a reflection boundary condition. In order to simulate the presence of weak horizons in a pre-existing basin in the foreland, we set the shear stresses on the base to be zero at intermediate values of *x* (blue-shaded area on Fig. 5). This boundary condition is equivalent to the range over-riding a weak substrate, and has the effect of minimizing vertical gradients of horizontal velocity (Fig. 5). As such, the model behaviour in this region approximates that of a 'Thin-Viscous-Sheet' model (e.g. Houseman & England 1986; Flesch *et al.* 2001), flowing between areas where the flow is coupled to the base.

This model is designed to capture the key physical effects that would result from the propagation of a mountain range over a laterally variable lower boundary, and therefore is useful in investigating the first-order effects on range deformation and topography. We compare the results of this model with the kinematics and topography of the actively deforming Sulaiman Range. We note that the seismic deformation that does occur in the Sulaiman Range is likely

to provide a good representation of the geometry of the strain, but not the rate (as is the case in other better-studied fold-thrust belts, such as the Zagros Mountains of Iran (e.g. Nissen *et al.* 2011b)). While our viscous fluid model cannot reproduce topographic features on a scale related to a single seismic event ($\leq$10 km), we can compare the orientation of the resultant model horizontal strain rate field with that inferred from our observations of seismicity. It is well known that the heterogeneous nature of faulted rocks means that slip in individual earthquakes may not exactly represent the underlying stress state, or the strain calculated from a rheologically homogeneous model. However, the variation in slip vector orientations around the Sulaiman Range is much larger than could result from such effects. We compare our model results to this first-order range-scale (i.e. $\geq$100 km) variation in the orientation of active deformation, and not the more minor local heterogeneities.

### 5.3 Model results

Cross-sections through the model mountain range after an elapsed time of 15 Ma (shown in Fig. 6) reveal that while the entire range front has advanced in the *y*-direction, the portion in the centre, overriding the shear-stress-free lower boundary, has propagated much further than the portion at either side, where the basal horizontal velocity is constrained to be zero (Fig. 6b). This is similar to the geometry of Sulaiman Range, which has formed a wide lobe, compared to the adjacent thinner fold-thrust belts (e.g. Kirthar Range), which have not. The model also produces similar topographic gradients to those observed in the Sulaiman Range and the adjacent mountain ranges to the north and south; at the edges of the model domain the model ranges are thin and have steep topographic fronts, whereas in the centre there is a flat-topped lobe with steep range front on either side, and a gentle slope down the apex. These lateral differences in topographic slope are a direct consequence of the lateral variations in lower boundary condition; the gentle slopes form above the stress-free base, and the steep slopes where the range encounters a rigid lower boundary (e.g. McKenzie *et al.* 2000).

Cross-sections through the centre of the model topography at successive time intervals during its evolution (Fig. 6c) reveal that as the range front advances, the range interior maintains a very low surface gradient while the initial steep topographic front that we imposed becomes gentler with time. This lessening of the gradient of the nose of the flow demonstrates that the topography we have seen in our models results from the presence of the laterally variable lower boundary condition, and not our initial conditions.

The horizontal surface velocity field shows significant horizontal variations due to the lateral change in basal boundary condition (Fig. 6a). On the margins of the model (where we impose zero basal horizontal velocity) the flow is strongly coupled to the base and the magnitude of the surface velocity is small; in the centre of the model (where we impose zero basal horizontal shear stress) the flow can slip freely over the base and so much larger surface velocities are observed. In this central portion of the range the velocities are limited by drag from the slower-moving regions on the lateral edges of the range, resulting in the most rapid velocities being in the centre of the mountain belt.

The horizontal strain rate tensor (Fig. 6a) shows that at the surface the model mountain range is undergoing little or no horizontal strain towards the back and centre of the range, but strong compressive strain towards the nose, and there are regions of equal compressive and extensional horizontal strain rate on either side (equivalent to horizontal shear on vertical planes, i.e. strike-slip faulting). This pattern is similar to that revealed by the seismicity of the Sulaiman Range; we observe thrust faulting around the nose (Fig. 3), an aseismic interior, and strike-slip faulting [e.g. the left-lateral Kingri Fault (Fig. 1b)] and en echelon folding on the east and west margins. The orientation of the maximum compressive strain rate axes fan out round the model range front and are oblique to it, as is the case for the thrust slip vectors in the Sulaiman Range (Fig. 3). At the margins of the model, where basal horizontal velocity is constrained to be zero, the compressive strain rate axes are orientated perpendicular to the range front. This matches the direction of thrusting observed in the Kirthar Range. In models with no along-strike variation in the basal boundary conditions, this pattern is present across the whole model—equivalent to there being no Sulaiman lobe and the thin Kirthar Range extending the whole way along the western border of the Pakistani lowlands.

## 6 DISCUSSION

Sarwar & De Jong (1979), Banks & Warburton (1986) and Humayon *et al.* (1991) previously suggested that the Sulaiman Range advances over weak sediments, and Macedo & Marshak (1999) proposed that the propagation of Sulaiman fold-thrust belt is controlled by the presence of a pre-existing basin on the Indian foreland. These authors considered the Sulaiman Range to behave as a frictional wedge. Davis & Lillie (1994), however, argue that the thickness of the carbonate-rich sedimentary section allows for ductile deformation of the range and mechanical coupling to the underthrust Indian lithosphere. Here, we have brought together these ideas along with our observations of topography, seismicity and additional data from earthquake source modelling to produce a dynamic model of the Sulaiman Range. We have used numerical models, and compared the model surface velocity field, topography and horizontal strain rate with what we observe in the Sulaiman Range. Our analysis of earthquake focal mechanisms and topography indicates that the propagation of the Sulaiman Range over India is driven by gravitational forces acting on topographic contrasts. Our simple dynamic model implies that lateral variations in topographic slope around the Sulaiman Range, and the greater across-strike width of the range relative to adjacent fold-thrust belts, are controlled by relatively weak sediments in a pre-existing basin in the foreland that act to reduce shear stresses at the base of the range (Fig. 7).

Our work builds on the previous work of Bernard *et al.* (2000), and differs because of our inclusion of a laterally variable lower boundary condition on the propagating mountain range. Based upon new observations and compilations of gravity data (Fig. 2; Förste *et al.* 2011), the gravity anomalies within the lowlands of Pakistan imply that relatively strong Indian lithosphere is underthrusting the fold-thrust belts of western Pakistan. We have therefore chosen to model the mountain ranges as overlying this Indian lithosphere, rather than using the approach of Bernard *et al.* (2000), in which the base of the model everywhere has zero shear stress, and there are no vertical gradients in horizontal velocity (i.e. no underthrusting). We also consider the evolution of our model topography with time, and compare this to the present-day topography of the Sulaiman Range, which was not undertaken by Bernard *et al.* (2000). Our model is in agreement with that of Bernard *et al.* (2000) on the importance of gravitational driving forces. Our additional conclusions regarding the role of the pre-existing basin on the Indian shield stem from the differences described above.

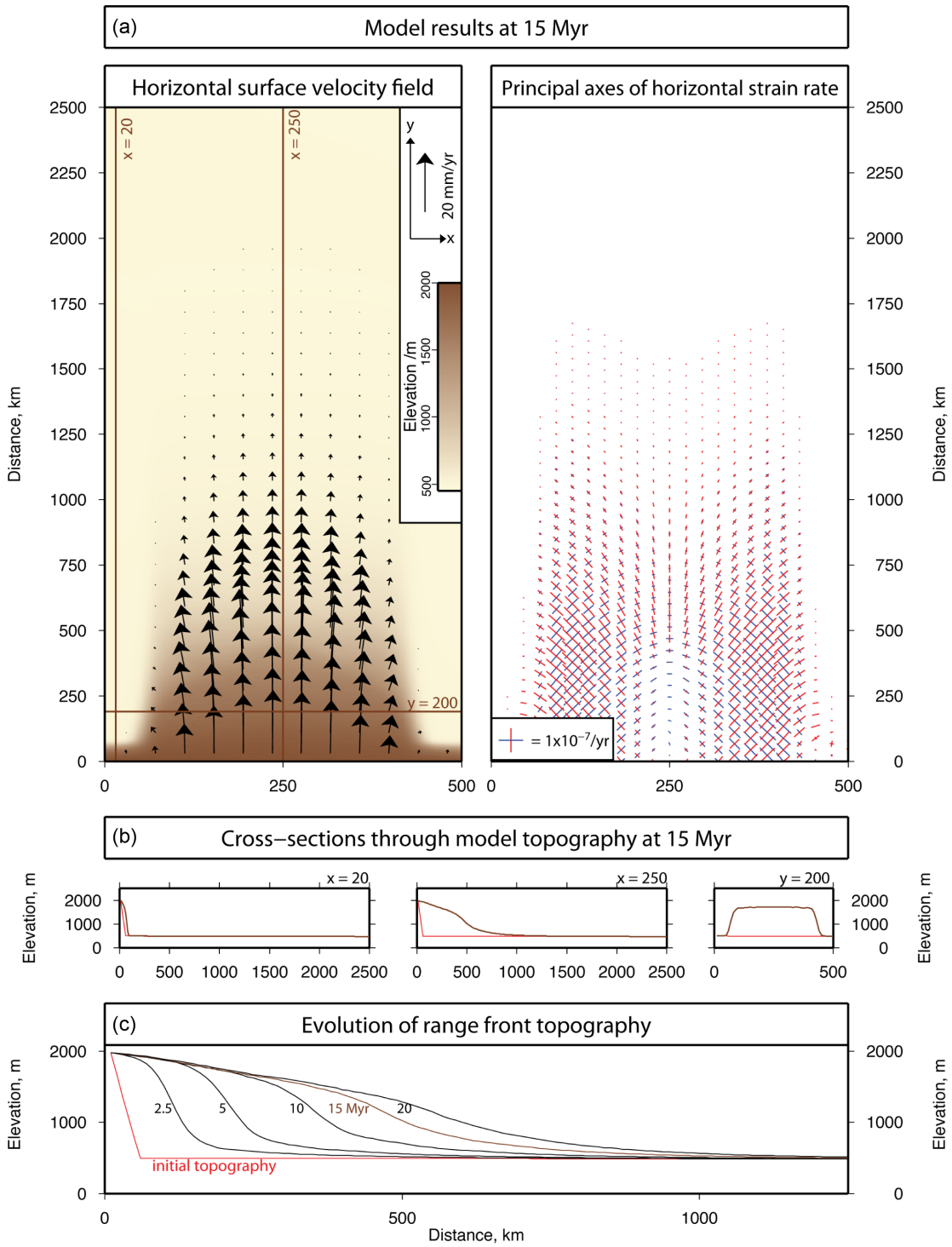


**Figure 6.** Model results at 15 Myr (a). Left-hand panel: horizontal surface velocity field (black arrows) overlain on model topography. Right-hand panel: Principal axes of horizontal strain rate. Red and blue lines are principal axes of compressive and extensional strain rate, scaled according to magnitude. (b) Cross-sections through model topography at $x = 20$ (across-strike, zero horizontal velocity at the base), $x = 250$ (across-strike, zero shear stress on the base) and $y = 200$ (along-strike). Initial topography shown in red, model topography at 15 Myr in brown. (c) Evolution of range front topography. Cross-sections through model topography at $x = 250$ after 2.5, 5, 10, 15 (brown) and 20 Myr. Initial topography in red.

In our model we do not attempt to include any complex geometric information about the size and shape of the postulated pre-existing sedimentary basin in the foreland. Given that the basin appears to be the main factor controlling the relative advancement of this fold-thrust belt in western Pakistan, it follows that the shape and lateral extent of this basin will control the direction in which the Sulaiman Range has propagated. We suspect that this effect governs second-order features of the Sulaiman Range, such as the asymmetry of the lobe, although there is insufficient data to justify adding this additional complexity to our models.

It is important to consider the effects of pre-existing basement topography on the behaviour of the Sulaiman Range. Fig. 1 shows

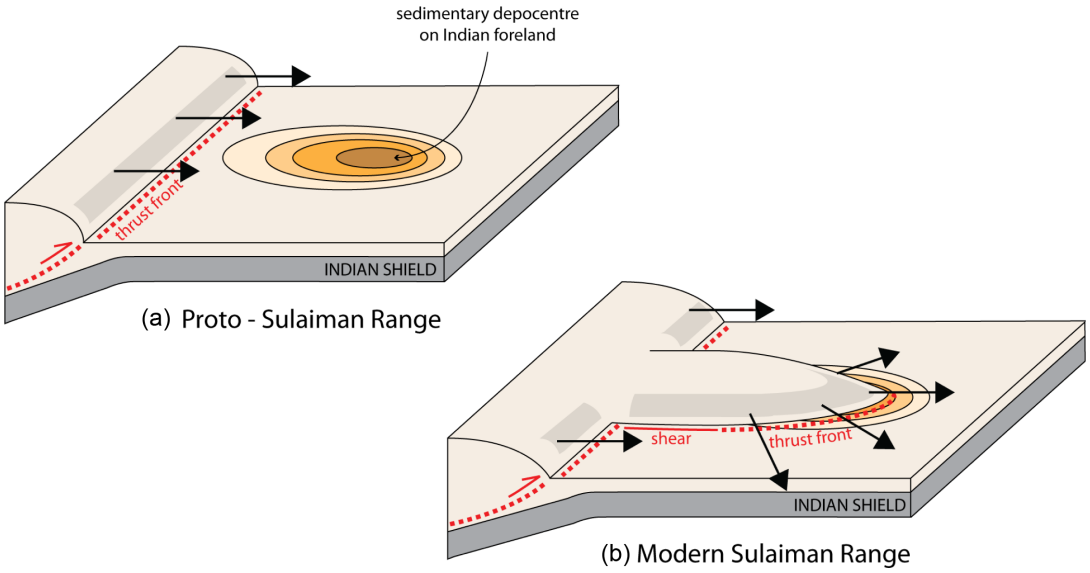


**Figure 7.** Summary cartoon of the development of the Sulaiman Range.

the spatial extent of basement highs known to exist outboard of the range; it should be noted their geometry is not well known. The Khairpur–Jacobabad high trends NNW–SSE, subparallel to the Sulaiman Range, though it is not known to extend underneath the thick sedimentary sequence within the mountains. Such basement features could lead to the development of lobate range fronts to mountain ranges propagating over thick sediments between basement highs. However, there are two lines of reasoning which suggest the influence of basement topography plays a minor role in the development of the Sulaiman Range when compared with the lateral variability of the lower boundary condition described above. Firstly, although basement topography could result in the presence of a lobate range front, without the presence of a laterally variable lower boundary the dramatic along-strike variations in surface slope would not be produced. Secondly, the ranges to either side of basement highs would be expected to propagate a similar distance in the absence of other factors. The anomalous extent of the Sulaiman Range compared with the other fold belts to the north and south suggests that other factors control the deformation, such as the laterally variable lower boundary condition that we model. Appendix C shows the results of a model which includes basement topography, but not lateral variability in the lower boundary condition, which illustrates these points (Supplementary material).

The Jacobabad High is a low, broad and relatively small feature of the basement relief, with a wavelength of ~100 km, a maximum amplitude of 1.3 km, limited surface expression (in the form of outcrops of Eocene rocks) and with up to 3 km sediments deposited on top (Hunting Survey Corporation Ltd 1960; Auden 1974; Raza *et al.* 1989, Fig. 1). It is positioned to the southwest of the Sulaiman Range, beyond the range front, rather than right in the apex of the Sibi syntaxis (as would be expected if it acted as a promontory impeding or diverting the advance of the fold-thrust belt). However, this basement high played an important role in forming discrete sedimentary basins in western Pakistan, in particular separating the depocentres for Jurassic–Tertiary sediments now uplifted in the Kirthar Ranges in the west and the Sulaiman Range in the east (Auden 1974; Smewing *et al.* 2002). Indeed, this may have been crucial in limiting the spatial extent of particular stratigraphic horizons, such as the weak shales or muds we propose control the advancement of the Sulaiman Range relative to the Kirthar Ranges. We therefore think that basement topography has only played an indirect role in governing the deformation, by limiting the area of deposition of the pre-existing basin on the Indian plate, and therefore giving rise to the lateral variation in geology and rheology that we model (Fig. 7).

In our dynamic model we allow material from an unseen reservoir to be drawn passively into the model domain, behind the advancing range front. This is equivalent to there being a reservoir of crust that can be drawn into the Sulaiman Range, i.e. the highlands of northeast Afghanistan (Fig. 2b). The curved fold axes that extend as far NW as the Katawaz basin (at ~68°E 32°N; Fig. 2) suggest that this motion is occurring, and that the structural fabric is being deformed by motion of crustal material into the Sulaiman Ranges from the NW. It is also possible that the ~30–40° bend in the Chaman Fault adjacent to the Sulaiman Range is related to this passive transport behind the propagating range. Such a style of boundary condition has previously been implemented in models of a variety of mountain ranges (e.g. Copley 2012), and implies that the material being drawn into the range has a similar effective viscosity as the propagating range, or is weaker.

Palaeomagnetic studies lend support to the dynamic model proposed in this paper. Klootwijk & Radhakrishnamurty (1981) find that uplifted Jurassic limestones in the central Sulaiman Range have rotated 50° clockwise relative to Indian basement since at least the middle Eocene, but possibly as late as the Plio-Pleistocene (Lawrence *et al.* 1981; Klootwijk 1984, Fig. 1b). This rotation is not observed in Kirthar Range to the southwest, nor at the young range front in the far eastern Fort Munro region. Rotations about vertical axes would be expected in the range interior in the model results shown in Fig. 6, with the same sense of rotation as observed by Klootwijk & Radhakrishnamurty (1981).

There are very few absolute dates available for the lithological units of the Sulaiman Range, and hence uncertainty on the age of the fold-thrust belt itself. This is compounded by the oblique nature of the collision and a limited understanding of the pre-collisional boundary configuration (Treloar & Izatt 1993; Qayyum *et al.* 1996). The dearth of surface velocity data, lack of knowledge of the stratigraphy at depth, and uncertainty about the age of the Sulaiman Range mean that we are unable to constrain its viscosity using our model. It should be noted, however, that the value of the viscosity does not

affect the behaviour or topographic evolution of the range, only the rate at which the range evolves. Biostratigraphic constraints from northern Pakistan (Beck *et al.* 1995), the timing of emplacement of ophiolites within the Sulaiman Range (Alleman 1979; Gnos *et al.* 1997) and Indian Plate motion reconstructions (e.g. Copley *et al.* 2010) put an upper bound of ∼55 Ma for the initial collision of India with Asia in the region of the Sulaiman Range. Age constraints from faunal assemblages in the Katawaz Basin sediments of the northwestern Sulaiman Range, together with structural observations from field mapping, suggest that the Sulaiman Range was uplifted in the early Miocene, and that the major period of deformation began before the Pliocene (Hunting Survey Corporation Ltd 1960; Humayon *et al.* 1991; Qayyum *et al.* 1997; Kassi *et al.* 2009; Kasi *et al.* 2012). If we take ∼10–55 Ma as the range of possible ages of the Sulaiman Range, then the average viscosity required to reproduce the observed topography is $10^{19}$–$10^{20}$ Pa s.

As discussed above, our model horizontal strain-rate field is consistent with the general spatial distribution of thrust and strike-slip earthquakes observed in the Sulaiman Range, and includes a zone of low strain rate in the interior of the model range comparable with the aseismic zone in the Sulaiman Range. However, our model shows strong compressive strain right at the front of the lobe, whereas significant thrust faulting earthquakes are absent from the immediate range front of the nose of the Sulaiman Range, and are instead set back from the range front. As the most recently uplifted part of the range, containing the youngest material, this is no surprise. Geological maps show that the nose of the Sulaiman Range and the area immediately ahead in the foreland are covered by recent molasse (Hunting Survey Corporation Ltd 1960), shed from the range front. The cover sequence of the Indian Shield is also comprised of a significant proportion of Indus floodplain gravels and clastic material shed from the Himalaya to the north (Qayyum *et al.* 2001). It is likely that much of the material in this area is not consolidated enough to be able to fail in earthquakes, hence the lack of seismicity. However, thickening and consolidation probably permits the seismic activity observed in a band across the nose, set back from the range front (Fig. 3). Further thickening and heating would result in the dominance of ductile deformation, as implied by the aseismic material to the north of the band of earthquakes.

For simplicity we used a constant-viscosity Newtonian fluid to model the Sulaiman Range. Using results from previous studies we can examine how our model results would change if more complex rheologies were used. The inclusion of non-Newtonian behaviour [used to model dislocation creep (e.g. Hirth & Kohlstedt 2003), and deformation on faults if the stress exponent is sufficiently large (e.g. Sonder & England 1986)] would change the details of the model results, but not the large-scale features we interpret. Non-Newtonian behaviour would focus the deformation into narrower zones, but the difference in topographic slope and deformation style between the areas with differing lower boundary conditions would be maintained (Gratton *et al.* 1999; Copley & McKenzie 2007). As discussed by Copley & McKenzie (2007), in the region with a stress-free base, the motions are governed by the layer in the overlying material which has the highest effective viscosity. For the case of a rigid base, the motions are governed by the viscosity structure within the entire thickness of the overlying material. Changes in the details of the viscosity structure can therefore make changes in the relative rates of propagation for a given rheological structure, but the features of the model we interpret here (the lateral variations in surface slope, and the location and orientation of the active deformation) are dominantly controlled by the lateral variation in lower boundary condition that we model.

The effects we discuss in the Sulaiman Range may be important elsewhere along the fold-thrust ranges of the Alpine-Himalayan belt. In the frontal portion of the Zagros Mountains of Iran, known as the Simply Folded Belt, much of the medium-magnitude seismicity occurs in the lower sedimentary cover and the thrust strikes follow the orientation of the range front (Nissen *et al.* 2011b). However, the GPS-derived convergence rate is only accounted for in part by the total seismic moment release across the range (Jackson & McKenzie 1988; Masson *et al.* 2005), therefore it is thought that aseismic processes are important in this fold-thrust belt (Nissen *et al.* 2011b). The deformation in the SFB is strongly influenced by the presence of Hormuz salt at the base of the cover sequence and evaporitic detachment horizons throughout (McQuarrie 2004; Sherkati *et al.* 2005). While the Sulaiman Range forms a wide lobe, the map-view geometry of the Zagros mountain front is much more linear. This is thought to be due to its large along-strike length resulting in curvature requiring a long time to develop (Copley 2012). Despite that, the range front does exhibit some second order sinuosity, with lobes and embayments on a scale of ∼200 km. These are thought to be due to the respective presence or absence of a basal salt layer (McQuarrie 2004; Nissen *et al.* 2011b), similar to the relatively weak Mesozoic sediments under the Sulaiman Range, and may have a similar effect in reducing the shear stress transmitted to the base of the deforming cover sequence by the rigid plate underneath.

## 7 CONCLUSIONS

(1) We present teleseismic body waveform inversion results for 10 moderate-sized earthquakes in the Sulaiman Range, showing that this is an active fold-thrust belt characterized by shallow thrust faulting close to the range front, strike-slip faulting towards the margins, and an aseismic interior. The seismicity appears to be restricted to the sedimentary sequence and does not involve the underthrusting Indian Shield.

(2) The fanning of thrust slip vectors around (and at an oblique angle to) the highly curved range front indicates that gravitational driving forces play a role in controlling the deformation. The propagation of this lobe, and the resulting topography, is likely to be controlled by the presence of low viscosity units in the pre-existing foreland cover sequence.

(3) Numerical modelling of the Sulaiman Range as a viscous flow propagating over a laterally variable base reproduces the first-order topography and geometry and generates a model surface velocity field and horizontal strain rate field compatible with the observed seismicity.

## ACKNOWLEDGEMENTS

This study forms part of the NERC- and ESRC-funded project ‘Earthquakes Without Frontiers’. Our thanks go to Jerome Neufeld for many interesting coffee-time discussions, and James Jackson and Dan McKenzie, for comments on the manuscript. We thank Chris Morley and one anonymous reviewer for helpful comments on the manuscript.

## REFERENCES

Abdel-Gawad, M., 1971. Wrench movements in the Baluchistan Arc and relation to Himalayan-Indian Ocean tectonics, *Geol. soc. Am. Bull.,* **82**(5), 1235–1250.

Alleman, F., 1979. Time of emplacement of the Zhob Valley ophiolites and Bela ophiolites, in *Geodynamics of Pakistan,* pp. 215–242, eds Farah, A. & De Jong, K.A., Geological Survey of Pakistan.

Ambraseys, N. & Bilham, R., 2003a. Earthquakes in Afghanistan, *Seism. Res. Lett.,* **74**(2), 107–123.

Ambraseys, N. & Bilham, R., 2003b. Earthquakes and associated deformation in northern Baluchistan 1892–2001, *Bull. seism. Soc. Am.,* **93**(4), 1573–1605.

Argand, E., 1924. La tectonique de l'Asie, in *Conférence devant le congrès géologique international (XIIIe session), 1922,* Bruxelles, pp. 171–372.

Armbruster, J., Seeber, L., Quittmeyer, R. & Farah, A., 1980. Seismic network data from Quetta, Pakistan: the Chaman fault and the fault related to the 30 May 1935 earthquake, in *Proceedings of the International Committee on Geodynamics, Group 6,* Peshawar, Vol. 13, pp. 129–142.

Auden, J.B., 1974. Afghanistan-west Pakistan, *Geol. Soc., Lond., Spec. Publ.,* **4**(1), 235–253.

Avouac, J.-P. *et al.*, 2014. The 2013, Mw 7.7 Balochistan earthquake, energetic strike-slip reactivation of a thrust fault, *Earth planet. Sci. Lett.,* **391,** 128–134.

Banks, C.J. & Warburton, J., 1986. 'Passive-roof' duplex geometry in the frontal structures of the Kirthar and Sulaiman mountain belts, Pakistan, *J. Struct. Geol.,* **8**(3–4), 229–237.

Bannert, D.N., 1992. Structural Development of the Western Fold Belt, Pakistan, no. 80–81 in Geologisches Jahrbuch Reihe B, Bundesanstalt für Geowissenschaften und Rohstoffe und den Geologischen Landesämtern in der Bundesrepublik Deutschland, Hannover.

Barke, R., Lamb, S. & MacNiocaill, C., 2007. Late Cenozoic bending of the Bolivian Andes: new paleomagnetic and kinematic constraints, *J. geophys. Res.: Solid Earth,* **112**(B1), doi:10.1029/2006JB004372.

Batt, G.E. & Braun, J., 1999. The tectonic evolution of the Southern Alps, New Zealand: insights from fully thermally coupled dynamical modelling, *Geophys. J. Int.,* **136**(2), 403–420.

Beck, R.A. *et al.*, 1995. Stratigraphic evidence for an early collision between northwest India and Asia, *Nature,* **373,** 55–58.

Bendick, R. & Flesch, L., 2013. A review of heterogeneous materials and their implications for relationships between kinematics and dynamics in continents, *Tectonics,* **32**(4), 980–992.

Bendick, R., McKenzie, D. & Etienne, J., 2008. Topography associated with crustal flow in continental collisions, with application to Tibet, *Geophys. J. Int.,* **175**(1), 375–385.

Bernard, M., Shen-Tu, B., Holt, W.E. & Davis, D.M., 2000. Kinematics of active deformation in the Sulaiman Lobe and Range, Pakistan, *J. geophys. Res.,* **105**(B6), 13 253–13 279.

Carey, S.W., 1955. The orocline concept in geotectonics, *Proc. R. Soc. Tasmania,* **89,** 255–288.

Chun, K.-Y., 1986. Crustal block of the western Ganga Basin: a fragment of oceanic affinity?, *Bull. seism. Soc. Am.,* **76**(6), 1687–1698.

Copley, A., 2008. Kinematics and dynamics of the southeastern margin of the Tibetan Plateau, *Geophys. J. Int.,* **174,** 1081–1100.

Copley, A., 2012. The formation of mountain range curvature by gravitational spreading, *Earth planet. Sci. Lett.,* **351–352,** 208–214.

Copley, A. & McKenzie, D., 2007. Models of crustal flow in the India-Asia collision zone, *Geophys. J. Int.,* **169,** 683–698.

Copley, A., Avouac, J.-P. & Royer, J.-Y., 2010. India-Asia collision and the Cenozoic slowdown of the Indian Plate: implications for the forces driving plate motions, *J. geophys. Res.,* **115**(B3), B03410, doi:10.1029/2009JB006634.

Copley, A., Avouac, J.-P., Hollingsworth, J. & Leprince, S., 2011. The 2001 $M_w$ 7.6 Bhuj earthquake, low fault friction, and the crustal support of plate driving forces in India, *J. geophys. Res.,* **116,** B08405, doi:10.1029/2010JB008137.

Craig, T.J., Copley, A. & Jackson, J.A., 2012. Thermal and tectonic consequences of India underthrusting Tibet, *Earth planet. Sci. Lett.,* **353–354**(C), 231–239.

Dahlen, F.A., 1990. Critical taper model of fold-and-thrust belts and accretionary wedges, *Ann. Rev. Earth planet. Sci.,* **18,** 55–99.

Davis, D.M. & Engelder, T., 1985. The role of salt in fold-and-thrust belts, *Tectonophysics,* **119**(1–4), 67–88.

Davis, D.M. & Lillie, R.J., 1994. Changing mechanical response during continental collision: active examples from the foreland thrust belts of Pakistan, *J. Struct. Geol.,* **16**(1), 21–34.

DeMets, C., Gordon, R.G. & Argus, D.F., 2010. Geologically current plate motions, *Geophys. J. Int.,* **181**(1), 1–80.

Dewey, J.F., Shackleton, R.M., Chengfa, C. & Yiyin, S., 1988. The tectonic evolution of the Tibetan Plateau, *Phil. Trans. R. Soc. Lond., A: Math. Phys. Sci.,* **327**(1594), 379–413.

Eames, F.E., 1951. A contribution to the study of the Eocene in western Pakistan and western India: A. The geology of standard sections in the western Punjab and in the Kohat district, *Quart. J. Geol. Soc.,* **107**(1–4), 159–171.

Ellis, S., 1996. Forces driving continental collision: reconciling indentation and mantle subduction tectonics, *Geology,* **24**(8), 699–702.

Engdahl, E.R., van der Hilst, R.D. & Buland, R., 1998. Global teleseismic earthquake relocation with improved travel times and procedures for depth determination, *Bull. seism. Soc. Am.,* **88**(3), 722–743.

England, P. & Houseman, G., 1988. The mechanics of the Tibetan Plateau [and discussion], *Phil. Trans. R. Soc. Lond., A: Math. Phys. Sci.,* **326**(1589), 301–320.

England, P. & McKenzie, D., 1982. A thin viscous sheet model for continental deformation, *Geophys. J. Int.,* **70**(2), 295–321.

Farah, A., Abbas, G., De Jong, K.A. & Lawrence, R.D., 1984. Evolution of the lithosphere in Pakistan, *Tectonophysics,* **105,** 207–227.

Flesch, L.M., Haines, A.J. & Holt, W.E., 2001. Dynamics of the India-Eurasia collision zone, *J. geophys. Res.,* **106**(B8), 16 435–16 460.

Förste, C. *et al.*, 2011. EIGEN-6—a new combined global gravity field model including GOCE data from the collaboration of GFZ-Potsdam and GRGS-Toulouse, in *Proceedings of the EGU General Assembly Conference Abstracts,* Geophysical Research Abstracts, Vol. 13.

Förste, C. *et al.*, 2013. EIGEN-6C2—a new combined global gravity field model including GOCE data up to degree and order 1949 of GFZ Potsdam and GRGS Toulouse, in *Proceedings of the EGU General Assembly Conference Abstracts,* Vienna, Austria, Geophysical Research Abstracts, Vol. 15, EGU2013-4077-1, p. 4077.

Gnos, E., Immenhauser, A. & Peters, T., 1997. Late Cretaceous/early Tertiary convergence between the Indian and Arabian plates recorded in ophiolites and related sediments, *Tectonophysics,* **271**(1–2), 1–19.

Gratton, J., Minotti, F. & Mahajan, S.M., 1999. Theory of creeping gravity currents of a non-Newtonian liquid, *Phys. Rev. E,* **60**(6), 6960–6967.

Griesbach, C.L., 1893. Notes on the earthquake of Baluchistan on the 20th December 1892, *Rec. Geol. Surv. India,* **26,** 57–64.

Haq, S.S.B. & Davis, D.M., 1997. Oblique convergence and the lobate mountain belts of western Pakistan, *Geology,* **25**(1), 23–26.

Hindle, D. & Burkhard, M., 1999. Strain, displacement and rotation associated with the formation of curvature in fold belts; the example of the Jura arc, *J. Struct. Geol.,* **21**(8–9), 1089–1101.

Hirth, G. & Kohlstedt, D., 2003. Rheology of the upper mantle and the mantle wedge: a view from the experimentalists, in *Inside the Subduction Factory, Geophysical Monograph 138,* pp. 83–105, ed. Eiler, J., Wiley Online Library.

Houseman, G. & England, P., 1986. Finite strain calculations of continental deformation: 1. Method and general results for convergent zones, *J. geophys. Res.,* **91**(B3), 3651–3663.

Humayon, M., Lillie, R.J. & Lawrence, R.D., 1991. Structural interpretation of the eastern Sulaiman foldbelt and foredeep, Pakistan, *Tectonics,* **10**(2), 299–324.

Hunting Survey Corporation Ltd 1960. *Reconnaissance geology of part of west Pakistan: a Colombo Plan Cooperative project,* Government of Canada (for the Government of Pakistan), Toronto.

Huppert, H.E., 1982. Propagation of two-dimensional and axisymmetric viscous gravity currents over a rigid horizontal surface, *J. Fluid Mech.,* **121,** 43–58.

Isacks, B.L., 1988. Uplift of the central Andean plateau and bending of the Bolivian orocline, *J. geophys. Res.: Solid Earth (1978–2012),* **93**(B4), 3211–3231.

Jackson, J.A. & McKenzie, D., 1984. Active tectonics of the Alpine-Himalayan Belt between western Turkey and Pakistan, *J. geophys. Res.,* **77,** 185–264.

Jackson, J.A. & McKenzie, D., 1988. The relationship between plate motions and seismic moment tensors, and the rates of active deformation in the Mediterranean and Middle East, *Geophys. J. Int.,* **93**(1), 45–73.

Jackson, J.A., McKenzie, D., Priestley, K. & Emmerson, B., 2008. New views on the structure and rheology of the lithosphere, *J. Geol. Soc.,* **165**(2), 453–465.

Jacob, K.H. & Quittmeyer, R.C., 1979. The Makran region of Pakistan and Iran: trench-arc system with active plate subduction, in *Geodynamics of Pakistan,* pp. 305–318, eds Farah, A. & De Jong, K.A., Geological Survey of Pakistan.

Jadoon, I.A.K., 1991. Thin-skinned tectonics on continent/ocean transitional crust, Sulaiman Range, Pakistan, *PhD thesis,* Oregon State University, OR.

Jadoon, I.A.K. & Khurshid, A., 1996. Gravity and tectonic model across the Sulaiman fold belt and the Chaman fault zone in western Pakistan and eastern Afghanistan, *Tectonophysics,* **254**(1–2), 89–109.

Jadoon, I.A.K., Lawrence, R.D. & Lillie, R.J., 1993. Evolution of foreland structures: an example from the Sulaiman thrust lobe of Pakistan, southwest of the Himalayas, *Geol. Soc., Lond., Spec. Publ.,* **74**(1), 589–602.

Kasi, A.K., Kassi, A.M., Umar, M. & Manan, R.A., 2012. Revised lithostratigraphy of the Pishin Belt, northwestern Pakistan, *J. Himalayan Earth Sci.,* **45**(1), 53–65.

Kassi, A.M., Kelling, G., Kasi, A.K., Umar, M. & Khan, A.S., 2009. Contrasting Late Cretaceous-Palaeocene lithostratigraphic successions across the Bibai Thrust, western Sulaiman Fold-Thrust Belt, Pakistan: their significance in deciphering the early-collisional history of the NW Indian Plate margin, *J. Asian Earth Sci.,* **35**(5), 435–444.

Kazmi, A.H., 1979. Active fault systems in Pakistan, in *Geodynamics of Pakistan,* pp. 285–294, eds Farah, A. & De Jong, K.A., Geological Survey of Pakistan.

Kazmi, A.H. & Rana, R.A., 1982. Tectonic Map of Pakistan.

Khan, M.A. *et al.*, 2008. Preliminary geodetic constraints on plate boundary deformation on the western edge of the Indian plate from TriGGnet (Tri-University GPS Geodesy Network), *J. Himalayan Earth Sci.,* **41,** 71–87.

Klootwijk, C.T., 1984. A review of Indian Phanerozoic palaeomagnetism: implications for the India-Asia collision, *Tectonophysics,* **105,** 331–353.

Klootwijk, C.T. & Radhakrishnamurty, C., 1981. Phanerozoic palaeomagnetism of the Indian Plate and the India-Asia collision, *Geodyn. Ser.,* **2,** 93–105.

Klootwijk, C.T., Nazirullah, R., De Jong, K.A. & Ahmed, H., 1981. A palaeomagnetic reconnaissance of northeastern Baluchistan, Pakistan, *J. geophys. Res.,* **86**(B1), 1–18.

Lamb, S. & Hoke, L., 1997. Origin of the high plateau in the central Andes, Bolivia, South America, *Tectonics,* **16**(4), 623–649.

Lawrence, R.D. & Yeats, R.S., 1979. Geological reconnaissance of the Chaman fault in Pakistan, in *Geodynamics of Pakistan,* pp. 351–358, eds Farah, A. & De Jong, K.A., Geological Survey of Pakistan.

Lawrence, R.D., Yeats, R.S., Khan, S.H., Farah, A. & De Jong, K.A., 1981. Thrust and strike slip fault interaction along the Chaman transform zone, Pakistan, *Geol. Soc., Lond., Spec. Publ.,* **9**(1), 363–370.

Macedo, J. & Marshak, S., 1999. Controls on the geometry of fold-thrust belt salients, *Geol. soc. Am. Bull.,* **111**(12), 1808–1822.

Marshak, S., 2004. Salients, recesses, arcs, oroclines, and syntaxes—a review of ideas concerning the formation of map-view curves in fold-thrust belts, in *Thrust Tectonics and Hydrocarbon Systems: AAPG Memoir 82,* pp. 131–156, ed. McClay, K.R., AAPG Special Volumes.

Masson, F., Chéry, J., Hatzfeld, D., Martinod, J., Vernant, P., Tavakoli, F. & Ghafory-Ashtiani, M., 2005. Seismic versus aseismic deformation in Iran inferred from earthquakes and geodetic data, *Geophys. J. Int.,* **160,** 217–226.

McCaffrey, R., Zwick, P. & Abers, G., 1991. SYN4 Program, *IASPEI Software Library,* **3,** 81–166.

McKenzie, D., Nimmo, F., Jackson, J.A., Gans, P.B. & Miller, E.L., 2000. Characteristics and consequences of flow in the lower crust, *J. geophys. Res.,* **105**(B5), 11 029–11 046.

McQuarrie, N., 2004. Crustal scale geometry of the Zagros fold–thrust belt, Iran, *J. Struct. Geol.,* **26**(3), 519–535.

Molnar, P. & Lyon-Caen, H., 1989. Fault plane solutions of earthquakes and active tectonics of the Tibetan Plateau and its margins, *Geophys. J. Int.,* **99,** 123–153.

MonaLisa & Jan, M. Q., 2010. Geoseismological study of the Ziarat (Balochistan) earthquake (doublet?) of 28 October 2008, *Curr. Sci.,* **98**(1), 50–57.

Nábělek, J. *et al.*, 2009. Underplating in the Himalaya-Tibet collision zone revealed by the Hi-CLIMB experiment, *Science,* **325**(5946), 1371–1374.

Nábělek, J.L., 1984. Determination of earthquake source parameters from inversion of body waves, *PhD thesis,* M. I. T., Dept. of Earth, Atmospheric and Planetary Sciences.

Nissen, E., Craig, T.J., McMullan, K., Parsons, B.E., Rickerby, A. & Wright, T.J., 2011a. The 27 February 1997 Sibi double-earthquake (Mw 6.9, 6.7) in the Sulaiman range of Pakistan—implications for the tectonics of fold-and-thrust belts and for earthquake triggering mechanisms, in *Proceedings of the AGU Fall Meeting Abstracts,* San Francisco, p. B8.

Nissen, E., Tatar, M., Jackson, J.A. & Allen, M.B., 2011b. New views on earthquake faulting in the Zagros fold-and-thrust belt of Iran, *Geophys. J. Int.,* **186,** 928–944.

Pattyn, F., 2003. A new three-dimensional higher-order thermomechanical ice sheet model: basic sensitivity, ice stream development, and ice flow across subglacial lakes, *J. geophys. Res.: Solid Earth,* **108**, 2382, doi:10.1029/2002JB002329.

Pezzo, G., Merryman Boncori, J.P., Atzori, S., Antonioli, A. & Salvi, S., 2014. Deformation of the western Indian Plate boundary: insights from differential and multi-aperture InSAR data inversion for the 2008 Baluchistan (Western Pakistan) seismic sequence, *Geophys. J. Int.,* **198**(1), 25–39.

Pinel-Puysségur, B., Grandin, R., Bollinger, L. & Baudry, C., 2014. Multi-faulting in a tectonic syntaxis revealed by InSAR: The case of the Ziarat earthquake sequence (Pakistan), *J. geophys. Res.: Solid Earth,* **119**(7), 5838–5854.

Press, W.H., Teukolsky, S.A., Vetterling, W.T. & Flannery, B.P., 2007. *Numerical Recipes,* 3rd edn, The Art of Scientific Computing, Cambridge Univ. Press.

Prevot, R., Hatzfeld, D., Roecker, S.W. & Molnar, P., 1980. Shallow earthquakes and active tectonics in eastern Afghanistan, *J. geophys. Res.,* **85**(B3), 1347–1357.

Qayyum, M., Niem, A.R. & Lawrence, R.D., 1996. Newly discovered Paleogene deltaic sequence in Katawaz basin, Pakistan, and its tectonic implications, *Geology,* **24**(9), 835–838.

Qayyum, M., Lawrence, R.D. & Niem, A.R., 1997. Molasse-delta-flysch continuum of the Himalayan orogeny and closure of the Paleogene Katawaz remnant ocean, Pakistan, *Int. Geol. Rev.,* **39**(10), 861–875.

Qayyum, M., Niem, A.R. & Lawrence, R.D., 2001. Detrital modes and provenance of the Paleogene Khojak Formation in Pakistan: implications for early Himalayan orogeny and unroofing, *Geol. Soc. Am. Bull.,* **113**(3), 320–332.

Quittmeyer, R.C. & Jacob, K.H., 1979. Historical and modern seismicity of Pakistan, Afghanistan, northwestern India, and southeastern Iran, *Bull. seism. Soc. Am.,* **69**(3), 773–823.

Raza, H.A., Ahmed, R., Ali, S.M. & Ahmad, J., 1989. Petroleum prospects sulaiman sub basin, pakistan, *Pak. J. Hydrocarb. Res.,* **1,** 21–56.

Reiter, K., Kukowski, N. & Ratschbacher, L., 2011. The interaction of two indenters in analogue experiments and implications for curved fold-and-thrust belts, *Earth planet. Sci. Lett.,* **302**(1–2), 132–146.

Rickerby, A.G., 2010. Multidisciplinary analysis of the 1997 Quetta earthquake, *Master's thesis,* Dept. of Earth Sciences, Bullard Laboratories, University of Cambridge, Cambridge.

Rowlands, D., 1978. The structure and seismicity of a portion of the southern Sulaiman Range, Pakistan, *Tectonophysics,* **51,** 41–56.

Royden, L., 1996. Coupling and decoupling of crust and mantle in convergent Orogens: implications for strain partitioning in the crust, *J. geophys. Res.: Solid Earth,* **101**(B8), 17 679–17 705.

Royden, L.H., Burchfiel, B.C. & van der Hilst, R.D., 2008. The geological evolution of the Tibetan Plateau, *Science,* **321**(5892), 1054–1058.

Rutter, E.H., 1983. Pressure solution in nature, theory and experiment, *J. Geol. Soc.,* **140**(5), 725–740.
Sarwar, G. & De Jong, K.A., 1979. Arcs, oroclines, syntaxes: the curvatures of mountain belts in Pakistan, in *Geodynamics of Pakistan,* pp. 341–350, eds Farah, A. & De Jong, K.A., Geological Survey of Pakistan.
Scholz, C.H., 1982. Scaling laws for large earthquakes: consequences for physical models, *Bull. seism. Soc. Am.,* **72**(1), 1–14.
Sherkati, S., Molinaro, M., Frizon de Lamotte, D. & Letouzey, J., 2005. Detachment folding in the central and eastern Zagros fold-belt (Iran): salt mobility, multiple detachments and late basement control, *J. Struct. Geol.,* **27**(9), 1680–1696.
Smewing, J.D., Warburton, J., Daley, T., Copestake, P. & Ul-Haq, N., 2002. Sequence stratigraphy of the southern Kirthar fold belt and middle Indus basin, Pakistan, *Geol. Soc., Lond., Spec. Publ.,* **195**(1), 273–299.
Sonder, L.J. & England, P., 1986. Vertical averages of rheology of the continental lithosphere: relation to thin sheet parameters, *Earth planet. Sci. Lett.,* **77**(1), 81–90.
Stein, S., Sella, G.F. & Okal, E.A., 2002. The January 26, 2001 Bhuj earthquake and the diffuse western boundary of the Indian Plate, in *Plate Boundary Zones,* pp. 243–254, eds Stein, S. & Freymueller, J.T., Geodynamics Series 30, American Geophysical Union.
Suárez, G., Molnar, P. & Burchfiel, B.C., 1983. Seismicity, fault plane solutions, depth of faulting, and active tectonics of the Andes of Peru, Ecuador, and southern Colombia, *J. geophys. Res.: Solid Earth (1978–2012),* **88**(B12), 10 403–10 428.
Szeliga, W., 2010. Historical and modern seismotectonics of the Indian Plate with an emphasis on its western boundary with the Eurasian plate, *PhD thesis,* University of Colorado, CO.
Szeliga, W., Bilham, R., Schelling, D., Kakar, D.M. & Lodi, S., 2009. Fold and thrust partitioning in a contracting fold belt: insights from the 1931 Mach earthquake in Baluchistan, *Tectonics,* **28**(5), 1–13.
Szeliga, W., Bilham, R., Kakar, D.M. & Lodi, S.H., 2012. Interseismic strain accumulation along the western boundary of the Indian subcontinent, *J. geophys. Res.,* **117**(B08404), doi:10.1029/2011JB008822.
Taymaz, T., Jackson, J.A. & McKenzie, D., 1991. Active tectonics of the north and central Aegean Sea, *Geophys. J. Int.,* **106**(2), 433–490.
Treloar, P.J. & Izatt, C.N., 1993. Tectonics of the Himalayan collision between the Indian Plate and the Afghan Block: a synthesis, *Geol. Soc., Lond., Spec. Publ.,* **74**(1), 69–87.
Vernant, P. *et al.*, 2004. Present-day crustal deformation and plate kinematics in the Middle East constrained by GPS measurements in Iran and northern Oman, *Geophys. J. Int.,* **157**(1), 381–398.
Wellman, H.W., 1966. Active wrench faults of Iran, Afghanistan and Pakistan, *Geol. Rund.,* **55**(3), 716–735.
Whitman, D., Isacks, B.L. & Kay, S.M., 1996. Lithospheric structure and along-strike segmentation of the Central Andean Plateau: seismic *Q*, magmatism, flexure, topography and tectonics, *Tectonophysics,* **259**(1), 29–40.
Yadav, R.B.S., Gahalaut, V.K., Chopra, S. & Shan, B., 2012. Tectonic implications and seismicity triggering during the 2008 Baluchistan, Pakistan earthquake sequence, *J. Asian Earth Sci.,* **45,** 167–178.
Zwick, P., McCaffrey, R. & Abers, G., 1994. MT5 Program, IASPEI software library.

## APPENDIX A: WAVEFORM INVERSION RESULTS

The minimum misfit solutions for waveform modelling of 10 events in the Sulaiman Range are presented in Figs A1–A10. Each figure is split into two panels; the upper showing all seismograms inverted for *P* waveforms, the lower those for SH waveforms. The title gives the date (yyyy-mm-dd) and moment magnitude of the event; the subtitle gives the focal mechanism parameters (strike/dip/rake/centroid depth/scalar moment) obtained via the inversion. Seismograms are labelled with the station name (e.g. NRIL) and alphabetic tag (e.g. A), assigned (in alphabetical order) according to azimuth, clockwise from north. Seismograms are plotted around the appropriate lower hemisphere projections of the focal sphere (*P* or *SH*) at their approximate station azimuth and the tag is plotted on the lower hemisphere projection at the point of intersection of the ray path. Observed seismograms are plotted with a solid line, synthetics with a dashed line, and the ticks mark the window of data used in the inversion. Black and white circles show the *P*- and *T*-axes, respectively. The amplitude scale (micrometres) is given to the bottom left of the focal sphere (N.B. for visual clarity, this may differ for *P* and *SH* waveforms). The source–time function (STF) is plotted under the *P* hemisphere, the seismogram timescale below.

Grey, starred station names indicate that the data was not used in the final inversion but are provided for comparison. For nodal planar stations, or stations with excessive noise, the direct arrivals are expected to have a very low amplitude compared to the background station noise, so it is not always possible to pick a direct arrival time for realigning the synthetic seismograms; often only the depth phases show clear arrivals in the broad-band data. In this case the seismograms are not included in the final inversion but are displayed to show the fit of the synthetics to the depth phases. The horizontal component data for stations TRI and MDT appears to be reversed in polarity compared with nearby stations for all the events we modelled. The seismograms from these stations have been flipped for display, but not included in the final inversion.

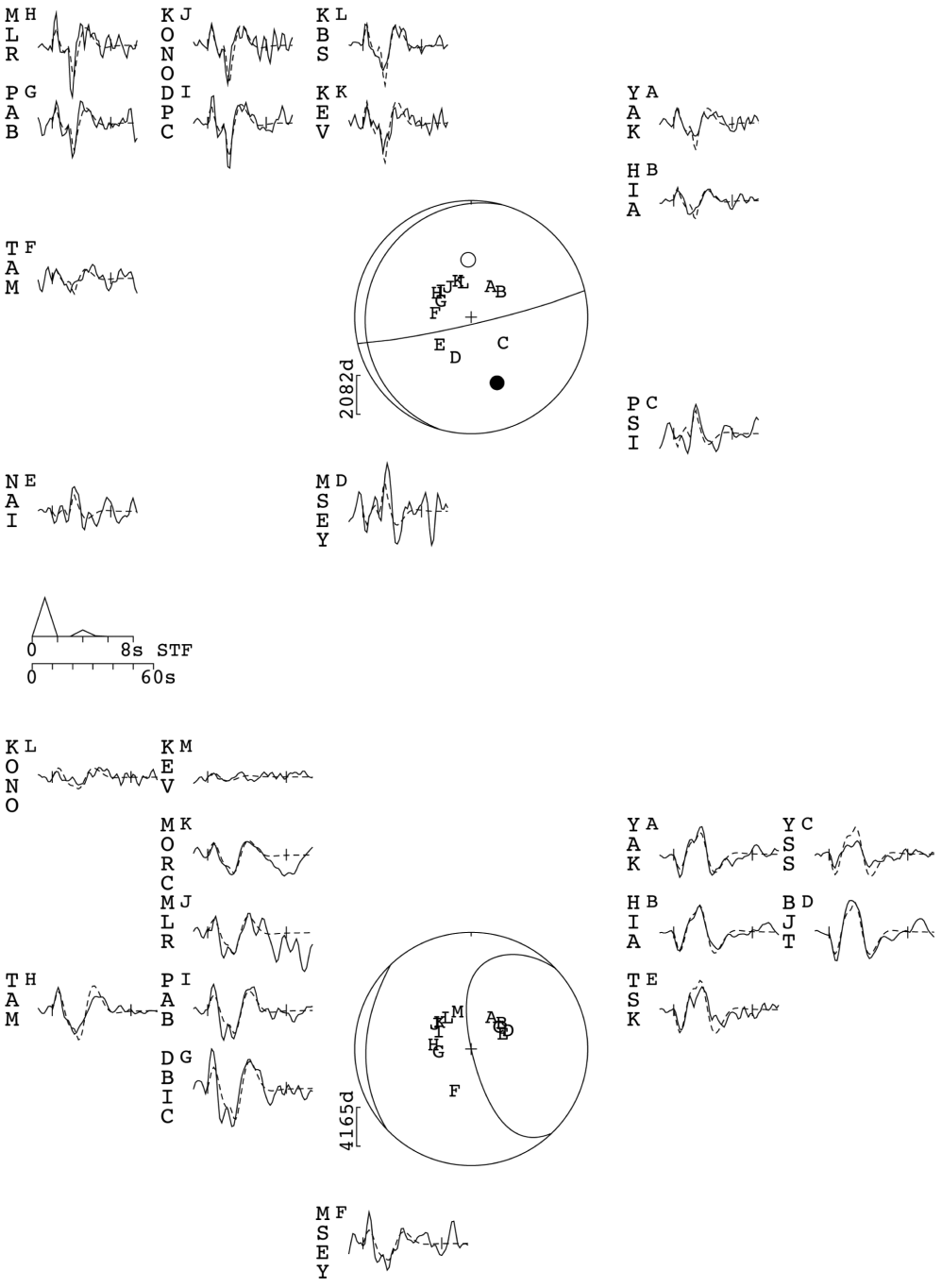


**Figure A1.** Minimum misfit solution for the earthquake of 31st May 1995.

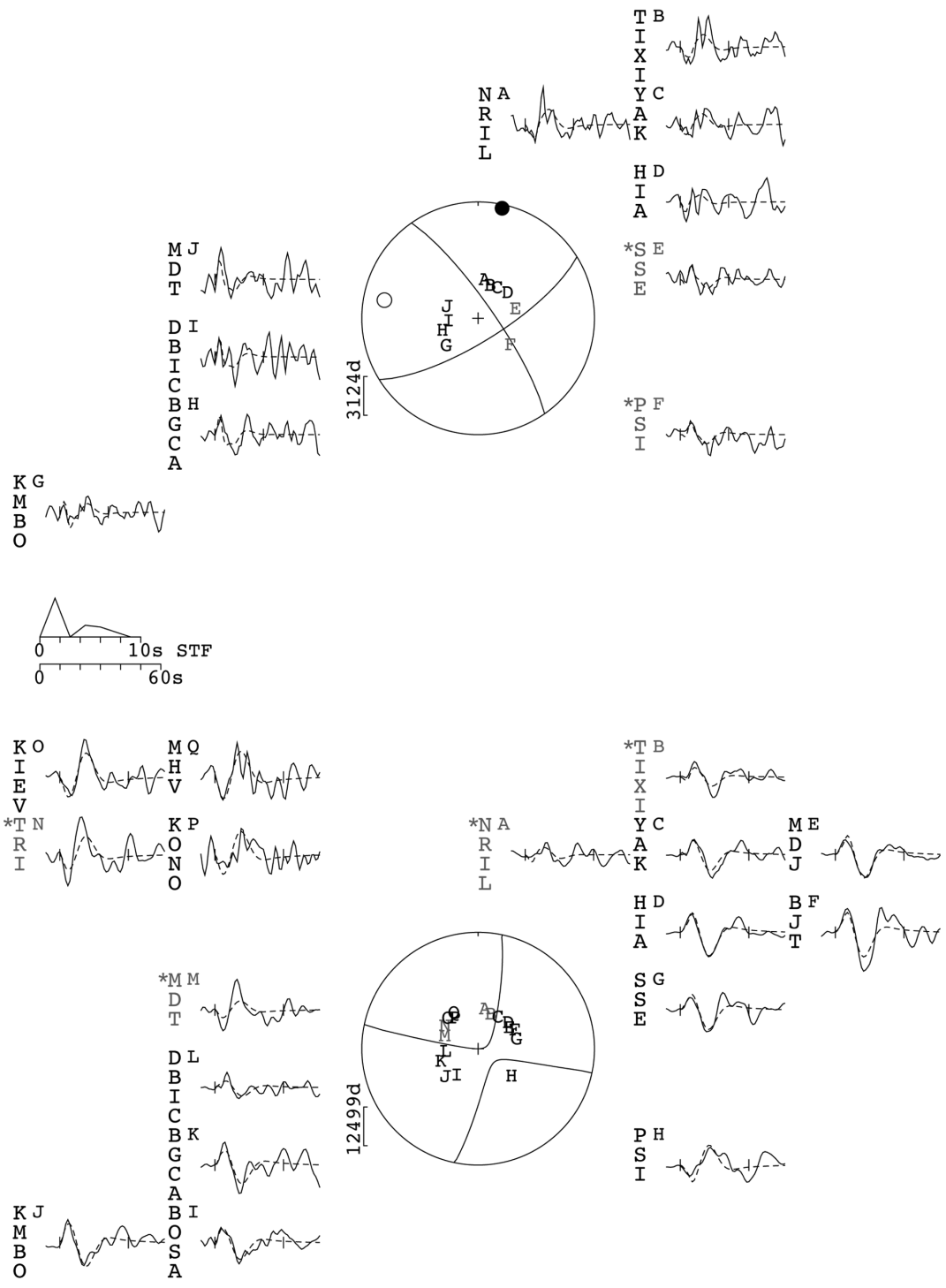


**Figure A2.** Minimum misfit solution for the earthquake of 4th March 1997.

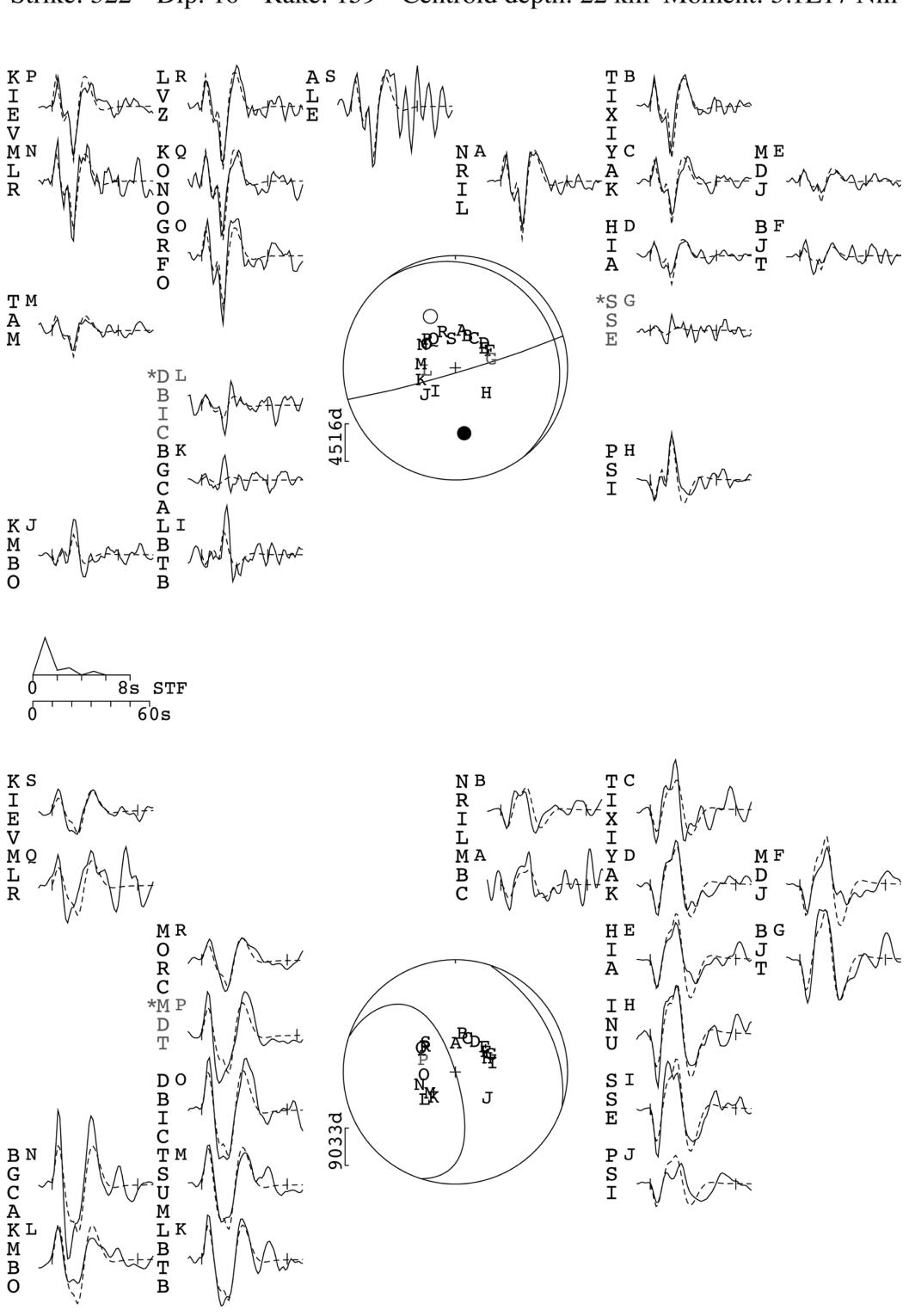


**Figure A3.** Minimum misfit solution for the earthquake of 20th March 1997.

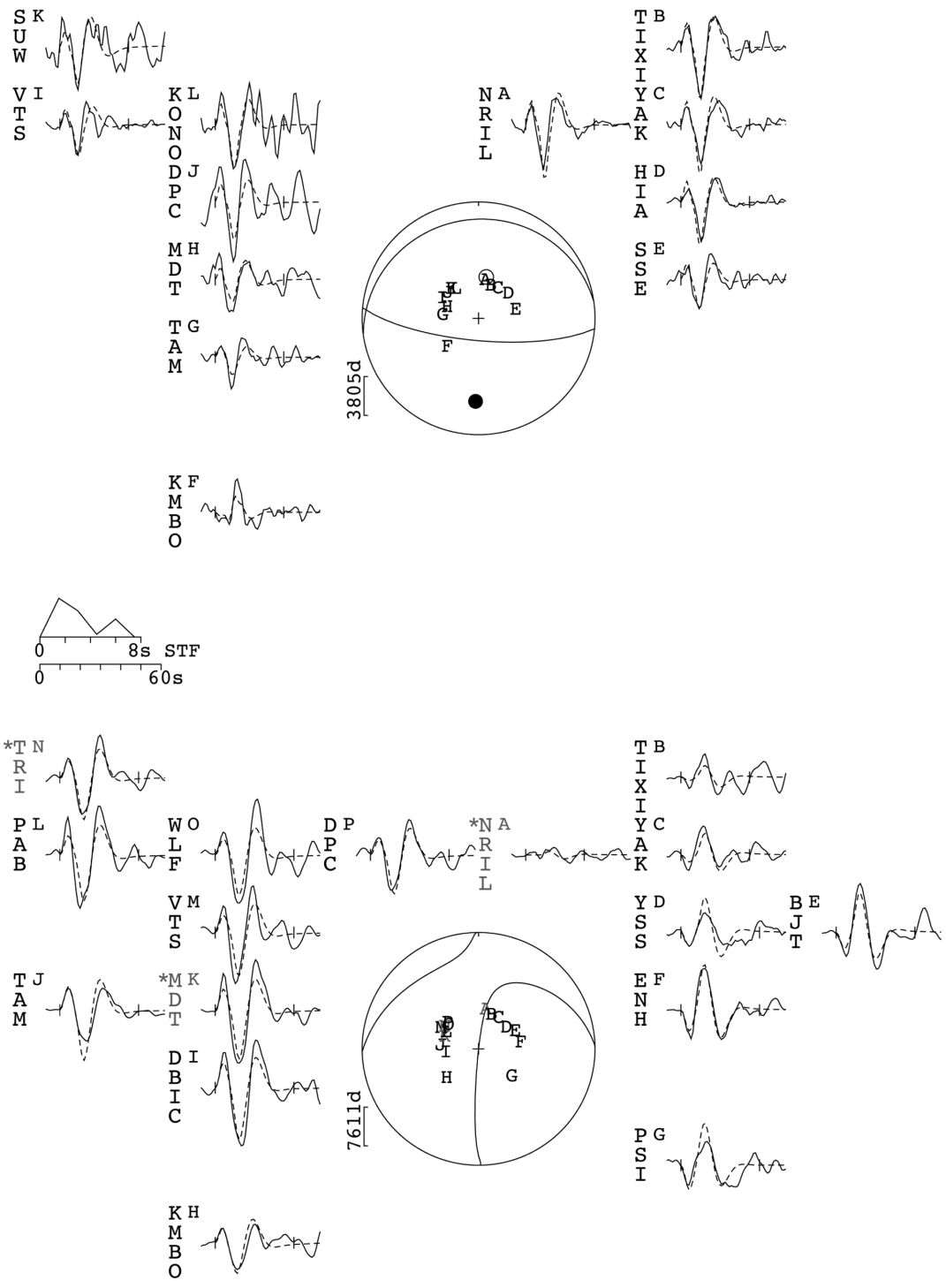


**Figure A4.** Minimum misfit solution for the earthquake of 24th August 1997.

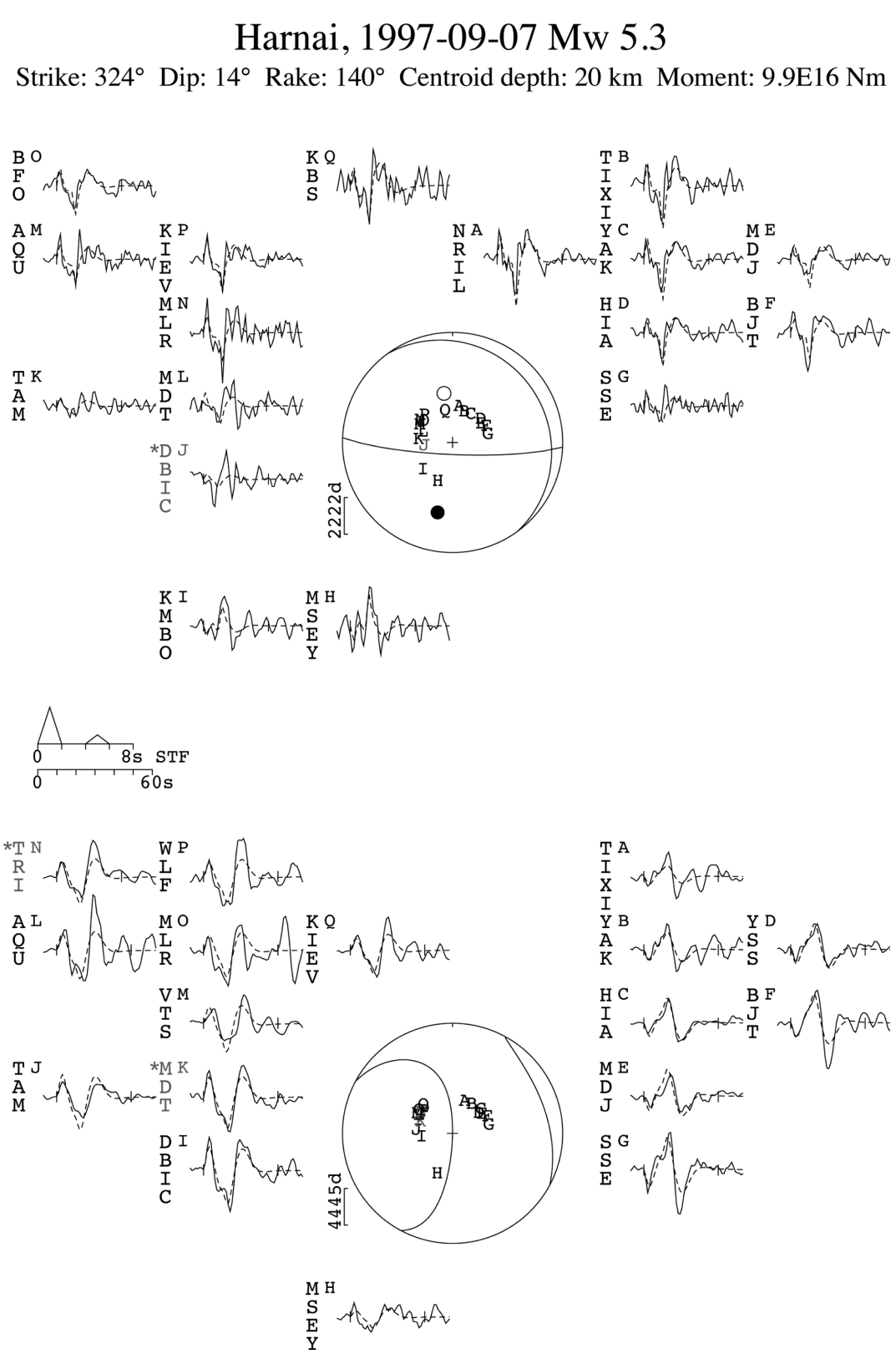


**Figure A5.** Minimum misfit solution for the earthquake of 7th September 1997.

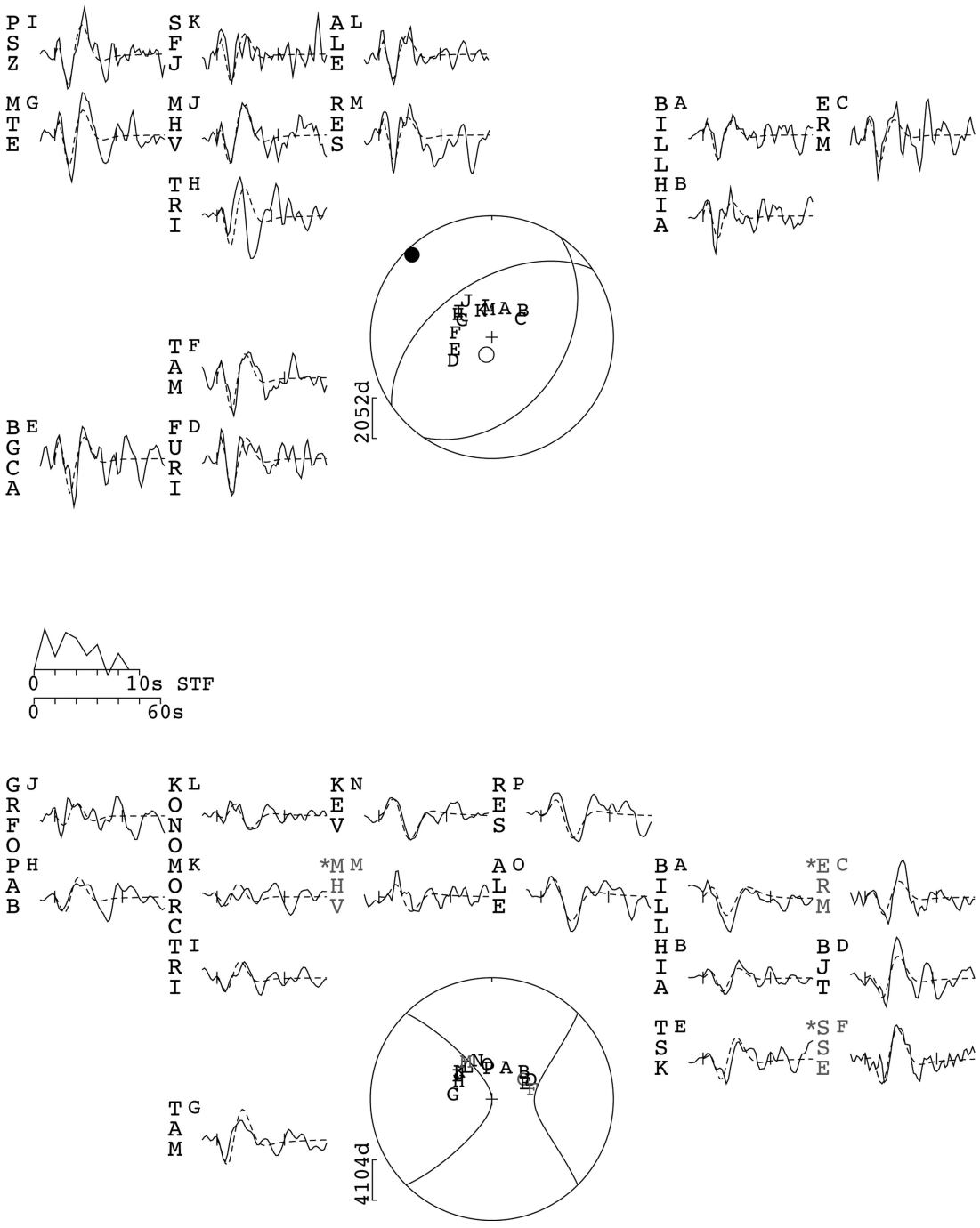


**Figure A6.** Minimum misfit solution for the earthquake of 26th June 1999.

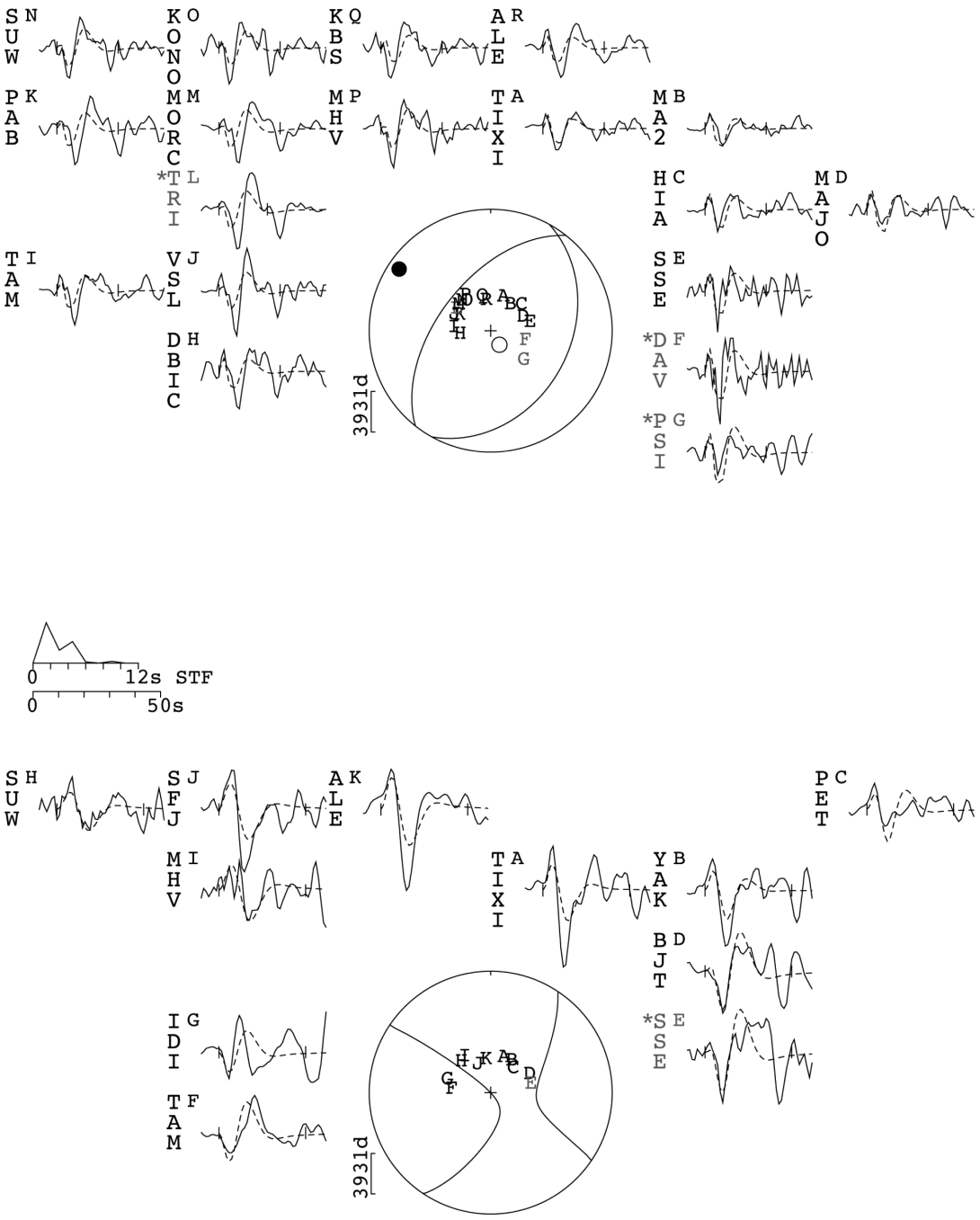


**Figure A7.** Minimum misfit solution for the earthquake of 12th July 1999.

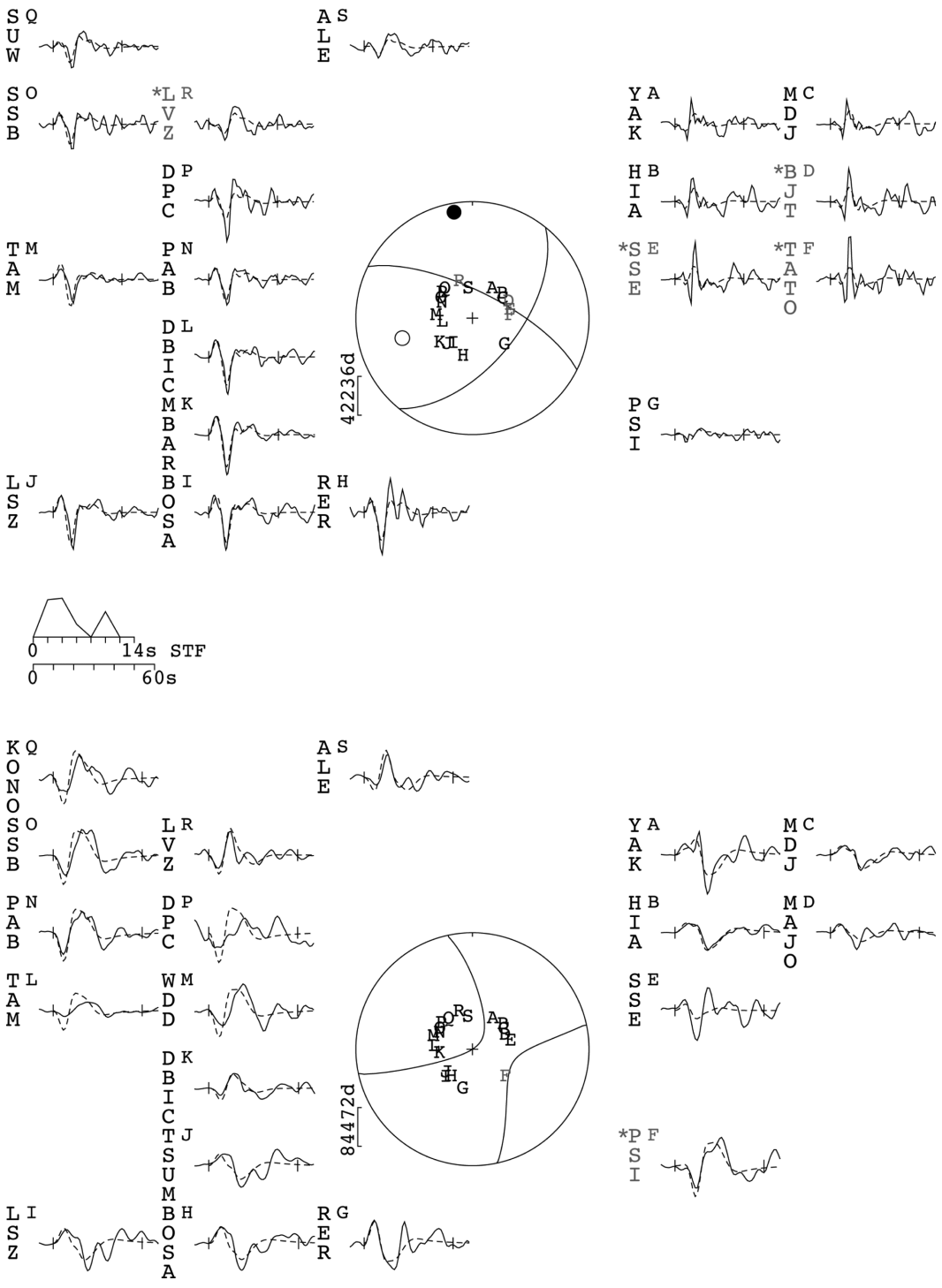


**Figure A8.** Minimum misfit solution for the earthquake of 28th October 2008.

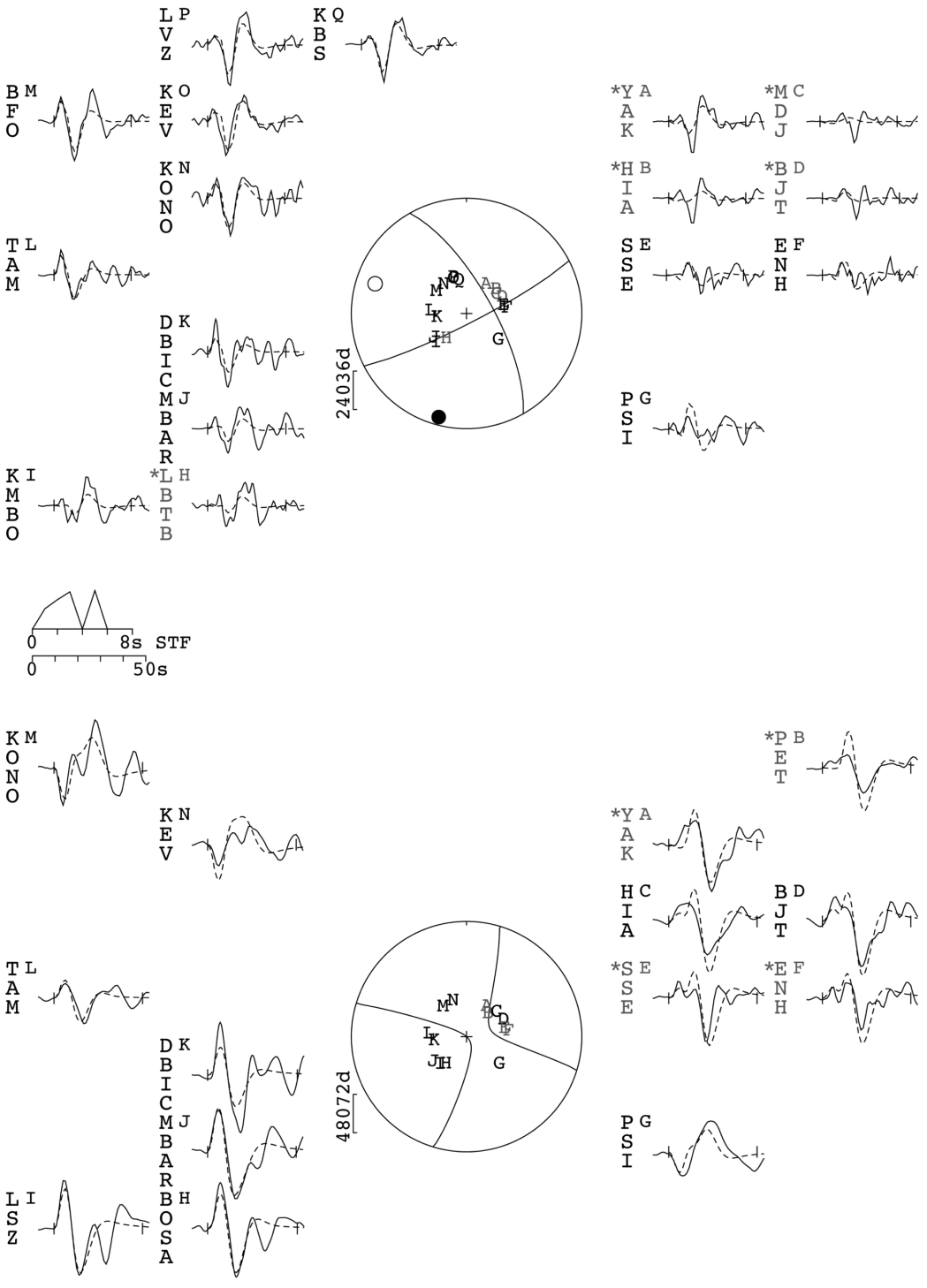


**Figure A9.** Minimum misfit solution for the earthquake of 29th October 2008.

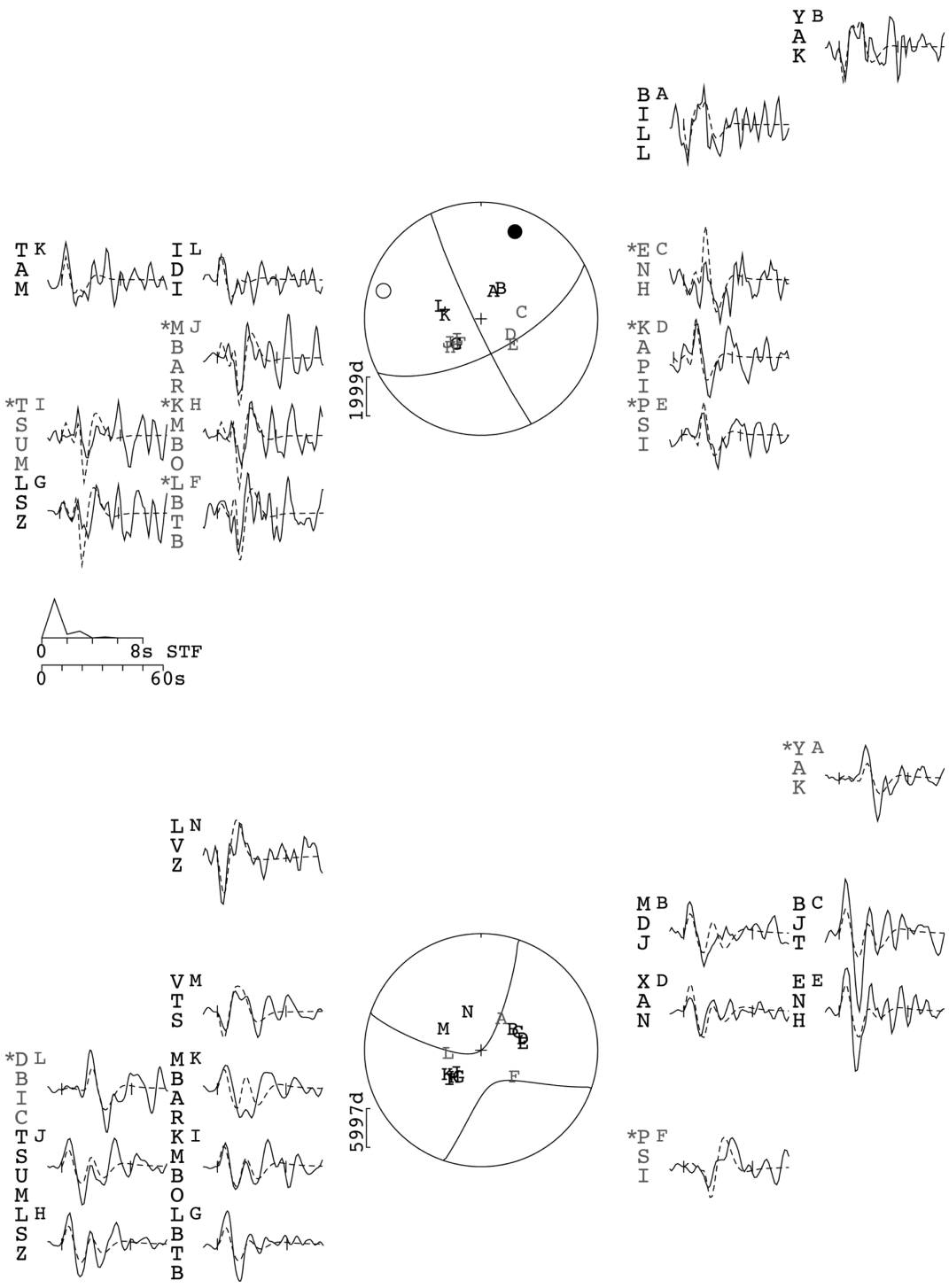


**Figure A10.** Minimum misfit solution for the earthquake of 9th December 2008.

## SUPPORTING INFORMATION

Additional Supporting Information may be found in the online version of this article:

**Appendix B.** Earthquake parameters.

**Appendix C.** Additional model results. (http://gji.oxfordjournals.org/lookup/suppl/doi:10.1093/gji/ggv005/-/DC1).

Please note: Oxford University Pres is not responsible for the content or functionality of any supporting materials supplied by the authors. Any queries (other than missing material) should be directed to the corresponding author for the article.